Economic Geology, v. 107, pp. 427–457

Hydrologic, Magmatic, and Tectonic Controls on Hydrothermal Flow, Taupo Volcanic Zone, New Zealand: Implications for the Formation of Epithermal Vein Deposits

Julie V. Rowland[1,†] and Stuart F. Simmons[2]

[1] *School of Environment, University of Auckland, Private Bag 92019, Auckland, New Zealand*

[2] *Hot Solutions Ltd, PO Box 32-125, Devonport, Auckland, New Zealand*

Abstract

Geologic controls on development of high-flux hydrothermal conduits that promote epithermal ore formation are evaluated at large and small scales for geothermal systems of the Taupo Volcanic Zone, New Zealand. Most geothermal systems occur within a rifted volcanic arc (~150 km long) dominated by silicic volcanism, and they occur in association with major faults near caldera structures or within accommodation zones that transfer extension between rift segments. The geothermal systems are hosted in a thick sequence (1–>3 km) of young volcanic deposits that rest unconformably on weakly metamorphosed Mesozoic argillite and graywacke. Flow regimes and permeability controls in one extinct (Ohakuri) and six active (Broadlands-Ohaaki, Waiotapu, Rotokawa, Waimangu, Te Kopia, and Orakeikorako) geothermal systems show that in general, hydrothermal fluid flow is controlled by (1) heat from magmatic intrusions which drives convective circulation; (2) intergranular host-rock porosity and permeability; (3) fault-fracture network permeability produced by tectonism, volcanism, and/or diking; (4) pipelike vertical conduits produced by volcanic and hydrothermal eruptions; and (5) hydrothermal alteration and mineral deposition that may cause heterogeneity in the porosity and permeability of a fluid reservoir. Such controls influence fluid flow within three distinctive depth zones: (1) a feed zone (>2,000 m depth), (2) an epithermal mineralization zone (<200–2,000 m depth), and (3) a discharge zone (0–200 m depth). Within the deepest part of the feed zone, hydrothermal fluid flow is influenced by magmatic intrusions guided by faults, which localize convection cells, and the brittle-ductile transition at the base of the seismogenic zone, which limits downflow of meteoric water. Hydraulic connectivity through low-permeability Mesozoic rocks is favored along NNE- to ENE- and WNW- to NNW-striking structures given the NW-SE direction of maximum extension (~10 mm/yr). In the epithermal mineralization zone, high-flux structures extend upward from the feed zone and transmit fluids to shallow depths, analogous to a geothermal production well. The host stratigraphic interval is dominated by porous pyroclastic deposits and distributed flow can be widespread until the intergranular permeability is reduced by hydrothermal alteration or where dense, low-porosity, high-tensile strength rocks exist. Distributed fluid-flow accounts for large volumes of hydrothermal alteration extending 10 to >100 km^3 that encloses geothermal reservoirs and high-flux fluid conduits. Fracture-dominated flow becomes important with decreasing porosity induced by hydrothermal alteration. In the discharge zone, the reduction in confining pressure, combined with mineral deposition and alteration, hydrothermal eruptions, and interplay of hot and cold waters create complex, but strongly localized flow paths that feed hot springs.

The permeability structure conducive to epithermal vein formation is analogous to a geothermal well: short in horizontal dimension (10s–100s m) but long in vertical dimension (>1,500 m) and possibly pipelike in shape. Episodic high-flux occurs over time scales of tens to thousands of years to accumulate sufficient amounts of gold and silver to form orebodies. During these episodes when faults and fractures are dilated, development of an upward-expanding column of boiling fluid promotes rapid ascent and high mass flow but also promotes silica and calcite precipitation, which can quickly reduce hydrothermal flow. Seismic activity and/or dike intrusion create and reactivate these high-flux pathways through extension and extensional shearing, caused by low differential stresses. The Taupo Volcanic Zone is highly prospective for epithermal-style mineralization, but the predominance of weak porous host rocks at shallow depths is prone to disseminated-style mineralization (e.g., Ohakuri). Structurally controlled mineralization forms in volcanic rocks where they have been embrittled by silicification through seismicity and fault displacement, caldera-forming eruptions, and dike intrusion.

Introduction

Geothermal activity in the central Taupo Volcanic Zone has long been associated with transport and deposition of gold, silver, and related trace metals, making the zone an important setting for investigating epithermal ore-forming processes. Most studies have focused on fluid chemistry, metalliferous precipitates, and related hydrothermal alteration (Grange, 1937; Weissberg, 1969; Browne, 1969; Henley and Ellis, 1983; Henley, 1985; Hedenquist and Henley, 1985; Brown, 1986; Krupp and Seward, 1987; Simmons and Browne, 2000, 2007; Reyes et al., 2003). Epithermal deposits nonetheless form in zones of high permeability in relatively shallow parts of geothermal systems, and bonanza ore grades are commonly localized within steeply dipping faults and fractures that were clearly channels of strongly focused hydrothermal fluid flow (e.g., Sillitoe, 1993). The patterns of zoned hydrothermal alteration that envelope these deposits also are affected by the conditions of fluid flow (e.g., Simmons et al., 2005). Accordingly, the physical attributes of the ore-forming environment are just as critical as the chemical attributes in determining the sites of precious metal mineralization and the extent and zoning of hydrothermal alteration. In this paper, we examine the physical controls on hydrothermal fluid flow for geothermal systems of the central Taupo Volcanic Zone (Fig. 1) and

[†] Corresponding author: e-mail, j.rowland@auckland.ac.nz

Submitted: April 23, 2010
Accepted: October 11, 2011

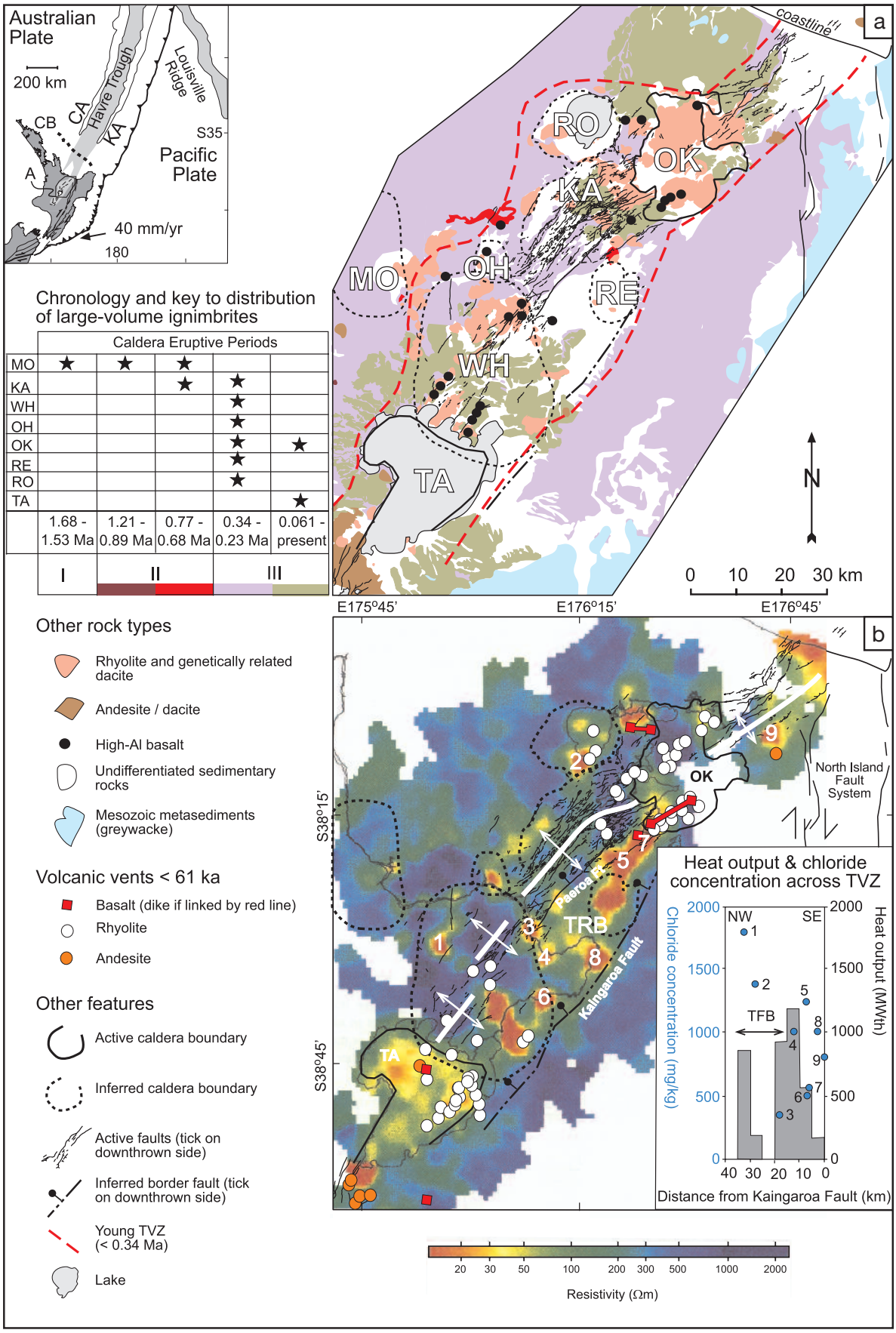
Australian Plate
200 km
CB
CA
Havre Trough
KA
Louisville Ridge
S35
Pacific Plate
A
40 mm/yr
180
a
coastline
RO
OK
KA
MO
OH
RE
WH
TA
N
0 10 20 30 km
E175°45'
E176°15'
E176°45'
b
S38°15'
S38°45'
North Island Fault System
Paeroa F.
TRB
Kaingaroa Fault
TFB
Heat output & chloride concentration across TVZ
Chloride concentration (mg/kg)
Heat output (MWth)
NW
SE
Distance from Kaingaroa Fault (km)
Chronology and key to distribution of large-volume ignimbrites
Caldera Eruptive Periods
1.68 - 1.53 Ma
1.21 - 0.89 Ma
0.77 - 0.68 Ma
0.34 - 0.23 Ma
0.061 - present
I
II
III
Other rock types
Rhyolite and genetically related dacite
Andesite / dacite
High-Al basalt
Undifferentiated sedimentary rocks
Mesozoic metasediments (greywacke)
Volcanic vents < 61 ka
Basalt (dike if linked by red line)
Rhyolite
Andesite
Other features
Active caldera boundary
Inferred caldera boundary
Active faults (tick on downthrown side)
Inferred border fault (tick on downthrown side)
Young TVZ (< 0.34 Ma)
Lake
20 30 50 100 200 300 500 1000 2000
Resistivity (Ωm)

interpret their significance relative to epithermal ore-forming processes.

We start with an overview of the volcanic and tectonic setting of geothermal activity in the Taupo Volcanic Zone followed by a description of the occurrences of high fluid-flow regimes and related gold-silver mineralization in six geothermal systems and one epithermal prospect (Fig. 2). The data comprise resistivity and geologic maps, which show the locations and extents of geothermal systems and their relationship to tectonic and volcanic structures, plus hydrologic information on deep flow rates, stratigraphic and structural controls on permeability, and the locations, discharges, and extents of surface hot spring activity. We use these to (1) assess the regional factors that localize geothermal systems; (2) show how lithology, structure, and hydrothermal alteration and mineral deposition control fluid movement through the epithermal environment in both space and time; and (3) evaluate factors conducive to development of high permeability fault-fracture conduits in an extensional environment. The last aim focuses on the formation of high-grade gold-silver–bearing epithermal veins, filled with quartz, adularia, and/or calcite gangue minerals.

For clarity a list of terms and definitions as used in this paper follow:

Geothermal system: A hydropressured[1] system involving convective circulation of water to >5 km depth driven by magmatic heat and centered on a rising column of hydrothermal fluid.

Geothermal field: The area of surface expression of hydrothermal activity in a geothermal system, represented by the distribution of warm and hot springs, fumaroles, geysers, and thermal ground.

Epithermal environment: The setting of hydrothermal, precious, and base metal ore formation in the shallow part of a geothermal system at <2 km depth and <300°C. Generally, epithermal mineralization forms at <1 km depth, but for the purposes of this paper we deepen it to encompass the vertical extent of boiling conditions in Taupo Volcanic Zone geothermal systems.

Permeability structure: The time-dependent network of interconnected pores and fractures that transmit fluid through rock over length scales in the hundreds to thousands of meters.

[1] Hydropressured refers to a fluid pressure gradient that is close to hydrostatic due to the weight of the overlying column of hot water.

Geologic Setting and Geothermal Systems of the Taupo Volcanic Zone

The Taupo Volcanic Zone developed within Mesozoic metasedimentary rocks (generically called graywacke and locally referred to as basement) over the last 2 m.y. in response to subduction of the Pacific Plate beneath the North Island of New Zealand (Fig. 1, inset). In its modern (<340 ka) form, the Taupo Volcanic Zone comprises a magmatically and structurally segmented rift system (Fig. 1: Wilson et al., 1995; Rowland and Sibson, 2001). Volcanism in northern and southern segments is dominated by cone-building eruptions of andesite, whereas the central segment is dominated by explosive eruptions of rhyolite, with calderas and rift basins infilling with more than 15,000 km^3 of air-fall deposits, ignimbrites, and lavas (Houghton et al., 1995; Wilson et al., 1995). Effusive rhyolite eruptions also formed many dome complexes in the central segment. Basalts occur rarely at the surface (<1% total volume of exposed volcanic rocks) but are presumably significant at midcrustal depths given the enormous natural heat flow through the central Taupo Volcanic Zone (Bibby et al., 1995; Wilson et al., 1995). The thermal power output of volcanic eruptions is only about 25% of the total thermal output of geothermal activity, and hydrothermal convection is the dominant mode of heat transfer on the time scale of ten thousands to hundred thousands of years (Hochstein, 1995).

Arrays of subparallel normal faults, together with vertical extension fractures and dike intrusion (Rowland and Sibson, 2001) accommodate about 10 mm/yr NW-SE extension across the central Taupo Volcanic Zone (Darby and Meertens, 1995; Wallace et al., 2004). These fault arrays define rift segments with ~20 km length scales. Transverse accommodation zones transfer extensional strain between adjacent rift segments (Fig. 1b). The predominance of parallel-striking normal faults, extension fractures, and dikes suggests a near-pure extensional tectonic regime within each rift segment, with vertical σ_1 = greatest principal stress, and horizontal σ_3 = least principal stress aligned NW-SE (Sibson and Rowland, 2003). Seismicity is dominated by widespread swarm activity with occasional moderate-to-large earthquakes (M_L <6.5; Bryan et al., 1999), defining a seismogenic zone 6 to 8 km deep. Focal mechanisms and an associated stress inversion also indicate a predominance of normal faulting with a subhorizontal σ_3 trending 148° (Hurst et al., 2002), nearly perpendicular to the strike of recently active faults (Rowland and Sibson, 2001).

FIG. 1. Geologic setting of geothermal activity in the Taupo Volcanic Zone. Inset: tectonic context of northern New Zealand (shaded mid-gray), location of (a) and region of back-arc rifting in the Havre trough. CA = Colville arc, CB = continental boundary, KA = Kermadec arc, Pacific-Australian Plate convergence shown in mm/yr. (a). Simplified geology of the central Taupo Volcanic Zone, showing faults, calderas, and distribution of major caldera-forming ignimbrites (color-coded according to age in table), and other rock types. Calderas: KA = Kapenga, MO = Mangakino, OH = Ohakuri, OK = Okataina, RE = Reporoa, RO = Rotorua, TA = Taupo, WH = Whakamaru. (b). Electrical resistivity of the central Taupo Volcanic Zone (nominal array spacing = 500 m: Stagpoole and Bibby, 1998), in relationship to <61 ka volcanic vents, rift segments, and inferred and active caldera boundaries (Nairn et al., 1994; Gravley et al., 2007). Rift axes defined by change in polarity of fault facing directions shown by white line and annotated with extension direction as defined by the pattern of active fault traces (Rowland and Sibson, 2001). Geothermal fields are indicated by low (<30 Ωm) resistivity (colored red). TRB = Taupo-Reporoa Basin, which is delimited by the Paeroa and Kaingaroa Faults to the west and east, respectively, and the Okataina and Taupo calderas to the north and south, respectively. Inset shows the heat outputs from geothermal systems, summed for 5 km wide strips parallel to the eastern margin of the Taupo Volcanic Zone (Bibby et al., 1995), and the concentrations of deep chloride waters supplying geothermal reservoirs—numbers correspond to geothermal systems located in map (Sheppard and Lyon, 1984; Giggenbach and Glover, 1992; Giggenbach, 1995; Simmons and Brown, 2007).

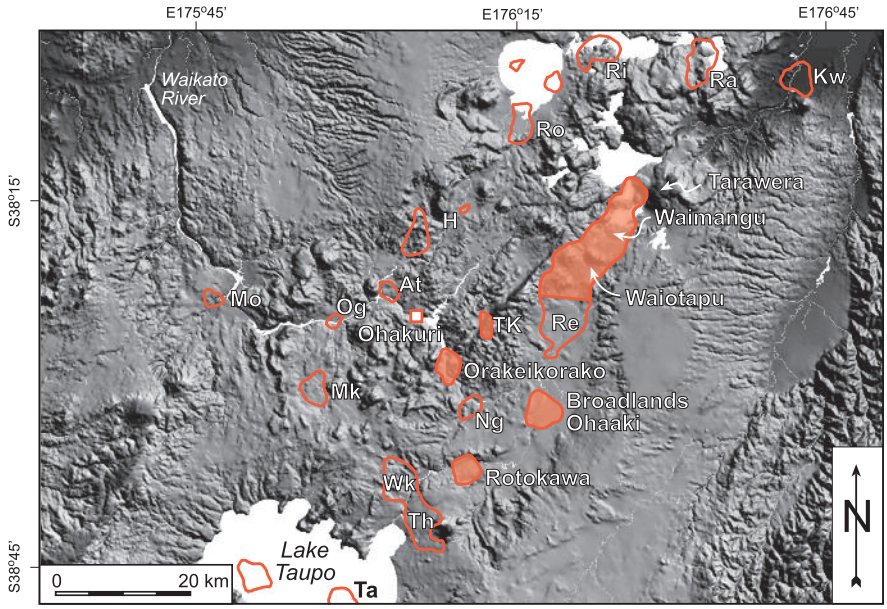

FIG. 2. Digital elevation model of the central Taupo Volcanic Zone, showing positions of geothermal systems, delimited by the 30 Ωm resistivity boundary (red outline; Bibby et al., 1995) and the extinct Ohakuri system (square box). Geothermal systems described in this paper are shaded red and labeled. Abbreviations are names of other geothermal systems (red outlines): At = Atiamuri, H = Horohoro, Kw = Kawerau, Mk = Mokai, Mo = Mangakino, Ng = Ngatamariki, Og = Ongaroto, Ra = Rotoma, Re = Reporoa, Ri = Rotoiti, Ro = Rotorua, Ta = Taupo, Th = Tauhara, TK = Te Kopia, Wk = Wairakei. Mount Tarawera shown for reference.

Approximately 10^8 t of hydrothermal water discharges annually from more than 20 geothermal systems (Bibby et al., 1995; Sibson and Rowland, 2003). Hydrothermal convection in geothermal systems is driven by buoyancy forces caused by the difference in density between the rising column of hot water and the surrounding column of cold water (e.g., Grant et al., 1982). As a result, meteoric water circulates to >5 km depth and transforms into a near-neutral pH chloride water, through incorporation of magmatic volatiles (H_2O, HCl, SO_2, H_2S, CO_2) and subsequent water-rock interaction, producing hydrothermal plumes that are distinguished on the basis of their physical and chemical characteristics (Bibby et al., 1995; Giggenbach, 1995). Thermal power outputs of individual geothermal systems range from <50 to 600 MW_{th}[2] (Bibby et al., 1995). Most of the geothermal systems are located between the two active silicic magmatic centers, Okataina and Taupo calderas (Fig. 1b). The typical 10 to 15 km spacing of geothermal systems is notably twice the seismogenic depth, which together with rheologic arguments suggests that fluid circulation extends the full depth of the seismogenic zone (McNabb, 1975; Bibby et al., 1995). The life spans of thermal activity of individual geothermal systems within the Taupo Volcanic Zone are poorly known but geologic evidence and one U-Th disequilibrium age date indicate they likely operate for 50,000 to 250,000 years (Browne, 1979; Grimes et al., 1998).

The position and footprint of Taupo Volcanic Zone geothermal systems can be delimited using images of electrical conductivity at shallow depth (<500 m; Bibby et al., 1995). Relationships between Taupo Volcanic Zone geothermal systems, Quaternary basins, and rift structure are shown in Figure 1. Two elongate zones of low resistivity extend from the Taupo caldera to the Okataina caldera parallel to the tectonic grain. These bound a densely faulted region on the west side of the central Taupo Volcanic Zone, which is notably devoid of present-day geothermal activity. The highest concentration of geothermal activity and convective heat transfer occurs within the Taupo-Reporoa Basin, a subsiding basin filled predominantly with thick (<5 km), poorly cohesive pyroclastic deposits and their reworked equivalents. Several zones of low resistivity trend perpendicular to the rift axes, coinciding spatially with accommodation zones and inferred NW-striking structures in the underlying graywackes (Wan and Hedenquist, 1981; Rowland and Sibson, 2004). The largest Taupo Volcanic Zone geothermal systems (Mokai, Rotorua, Waiotapu, Waimangu, Te Kopia, Orakeikorako, and Wairakei-Tauhara) occur near or on caldera structures or at the lateral tips of major faults.

Chloride waters containing 500 to 2,000 ppm Cl and 80 to 240 ppm H_2S are responsible for transporting large quantities of gold and silver. The large variation in gold (<0.1–~23 ppb) and silver (2.7–2,400 ppb) concentrations suggest that the supply of precious metals in deep hydrothermal solutions is controlled by the intrusion of andesitic and basaltic magmas, which also govern convective heat transfer and the hydrothermal fluxes of other metals (Simmons and Brown, 2007). The Rotokawa and Mokai geothermal systems have the highest hydrothermal gold and silver fluxes (Fig. 2), and they can supply enough metal in 50,000 years or less to match the inventories of the largest hydrothermal gold-silver deposits in the world (Simmons and Brown, 2007). However, the ore grade mineralization that has been found in the Taupo Volcanic Zone geothermal systems is mostly restricted

[2] $MW_{th} = MW_{thermal}$

to deposits in hot springs and production wells (e.g., Weissberg, 1969; Hedenquist and Henley, 1985; Brown, 1986; Simmons and Browne, 2000; Reyes et al., 2003).

The combination of boiling and focused fluid flow in a geothermal well is conducive to deposition and accumulation of large amounts of precious metals in a short period of time, representing conditions that lead to formation of epithermal veins (Henley, 1985; Brown, 1986; Simmons and Browne, 2000). Within a production well, fluid buoyancy results from decompressional boiling of an upward-expanding fluid column in which the mixture of steam and water accelerates upward, attaining very high velocity near the surface (Grant et al., 1982; Hedenquist and Henley, 1985). The thermal power output of individual wells is about 100 ± 50 MW_{th}, and flow is generally sustained by one, two, or three narrow feed points into the well (Donaldson and Grant, 1981; Grant et al., 1982). Fluid sucks into the well at the feed point because the weight of the dynamic flow column is less than the pressure of subboiling liquid contained in the surrounding geothermal reservoir. A feedback control on fluid flow thus develops between focused boiling in the well and the supply of hot water from the reservoir. These conditions form naturally and episodically where and when a suitable permeability structure develops, in the shallow upflow zone of the geothermal system where near-boiling pressure-temperature conditions exist. High-flux fluid conditions are transient and short-lived, which is a point we discuss at greater length below.

Fluid Flow in Taupo Volcanic Zone Geothermal Systems

A large body of information about Taupo Volcanic Zone geothermal systems has been gained since 1950 through deep drilling (~3 km depth), including (1) stratigraphy and structure of rocks hosting and enclosing reservoirs between 600 and 3,000 m depth; (2) fluxes, pressures, temperatures, and compositions of hydrothermal fluids; and (3) occurrences and zonations of hydrothermal minerals. We selected seven well-documented locations (Table 1, Fig. 2) to illustrate the diversity of epithermal flow regimes that exist in the central Taupo Volcanic Zone. Much of the insight regarding these flow regimes depends on surface data of thermal activity (hot springs, steaming ground, fumaroles, hydrothermal eruption vents) and exposures of uplifted and exhumed altered blocks that represent the shallow epithermal environment (<300 m depth), supplemented by data from a small number of scattered wells. For this reason, we begin with a review of the Broadlands-Ohaaki geothermal system (Figs. 2, 3), where a three-dimensional picture of the controls on fluid flow, inside and outside the epithermal environment, is best understood, and where hydrothermal fluids transport and deposit gold and silver.

Broadlands-Ohaaki

More than 50 geothermal wells were drilled (between 370 to 2,600 m deep) prior to commissioning of the Ohaaki power station in 1988. The well data provide most of the information about stratigraphy, thermal and chemical structure, hydrothermal alteration, and fluid flow within this system (Fig. 3a-c; Hedenquist, 1990; Simmons and Browne, 2000). A flat-lying layered sequence of Quaternary rhyolitic to dacitic, pyroclastic deposits and lavas (total thickness of 800 to >2,000 m) is underlain by block-faulted and weakly metamorphosed Mesozoic graywacke and argillite (Fig. 3b; Grindley and Browne, 1968; Browne, 1971; Wood, 1983; Henrys and Hochstein, 1990). There is no surface expression of faulting, and structural features are inferred from stratigraphic analysis of drill cuttings and core intervals. Major faults are located from offsets in the contact between the graywackes and overlying cover sequence. Faults appear to dip steeply and mostly strike NE, parallel to the structural grain of the Taupo Volcanic Zone (Grindley and Browne, 1968; Henrys and Hochstein, 1990).

The shape of isotherms marks two zones of fluid upflow of deeply derived chloride water rich in aqueous CO_2 (Fig. 3b; Hedenquist, 1990). The maximum vertical temperature gradient is in the center of the upflow zone, and it is represented by a hydrodynamic boiling curve in which water begins to boil at ~310°C and 2,000 m depth (Sutton and McNabb, 1977; Grant et al., 1982). The geothermal reservoir, which lies between 700 and 2,000 m depth, is hydraulically connected to the surrounding volume of rock filled with colder water. Temperature inversions occur locally above and on the margins of upflow zones, where relatively cool (~150°C) CO_2-rich steam-heated waters mix with ascending chloride water (Hedenquist, 1990). The complexity in the shallow hydrology is common to all drilled geothermal systems within the Taupo Volcanic Zone. The water table lies within a few meters of the surface due to high annual rainfall (1,260 mm/yr) and flat topography (290–330 m asl.). The only major surface thermal feature is the Ohaaki Pool (800 m^2), which lies along an inferred NE-striking fault (Grindley and Browne, 1968), and prior to drilling discharged 4 to 12 kg/s of 95°C mixed chloride-bicarbonate-type water (Weisberg, 1969). Surficial steam-heated acid-sulfate waters occur sporadically and are confined to <20 m depth.

Fluid movement is largely controlled by the buoyancy of the hydrothermal plume and the permeability structure, which distributes the fluid flow. Near-constant thermal gradients (laterally and vertically) have been established so that before production began hydrothermal fluid flow transferred heat energy to the surface and shallow aquifers where it was dissipated by mixing with cool groundwater. Local zones of high permeability are indicated by circulation losses during drilling, which are somewhat randomly distributed in the volcanic stratigraphy (Fig. 3b). Zones of extinct permeability are also indicated by relatively rare occurrences of veinlets (<1 cm wide) in cores, containing quartz, adularia and/or calcite (Browne, 1970, 1978; Grindley and Browne, 1976). The Ohaaki fault (Fig. 3b, c) is one of the few structures that is known to be a site of high permeability (Browne and Ellis, 1970). Drill holes penetrating graywacke have yet to encounter high permeability with hydrothermal fluid. In the overlying volcanic rocks, fluid flow is distributed laterally due to high permeability associated with interconnected pore space in pyroclastic units and their contacts (Grindley and Browne, 1976). Rock porosity in the volcanic sequence is highly variable, ranging between 10 and 40% and decreases with depth, whereas it is only ~5% in the underlying graywacke (Ministry of Works and Development, 1977; Brathwaite et al., 2002). Because of large-scale physical heterogeneities in the volcanic rocks, measurements of permeability on intervals of

Table 1. Character of the Epithermal Environment in Selected Geothermal Systems of the Taupo Volcanic Zone

Field (MW_{th})	Flow (kg/s)	Surface expression	Permeability controls	Stratigraphy	Structure	Surface footprint (km^2): 10 Ωm contour	Surface footprint (km^2): 30 Ωm contour	Mineralization	References
B-O (70)	100	Ohaaki Pool (800 m^2), chloride-bicarbonate spring with silica sinter, total flow ~10 kg/s	Anisotropic focused high-flux vertical flow over depth intervals >500 m in geothermal wells; lithologies and rock contacts form strong horizontal permeability within volcanic stratigraphy; fracture permeability presumed to dominate in basement graywacke	Horizontally bedded volcanic deposits 1 to >2 km thickness unconformably overlie Mesozoic graywacke basement	Inferred NE-trending faults in basement	9.25	22.6	Highest concentrations in geothermal wells (6 wt % Au, 30 wt % Ag) with chalcopyrite; disseminated Au (<1 ppm) and Ag (<10 ppm) occur in altered volcanic rocks <500 m depth; Au and Ag also deposited in Ohaaki Pool (1957–1958) with Hg, As, Sb, Tl, S	Grindley and Browne (1968), Browne (1969), Weissberg (1969), Browne and Ellis (1970), Brown (1986), Hedenquist (1990), Simmons and Browne (2000)
OH (extinct)	None	Silica sinter deposits and widespread alunite-kaolinite alteration indicate the former discharge of near-neutral pH chloride springs and steam-heated acid sulfate waters	Predominantly distributed permeability in porous pyroclastic deposits, followed by weak fracture control as a result of intense silicification	Bedded rhyolitic pyroclastic deposits				Subeconomic disseminated Au-Ag mineralization associated with intense quartz-adularia alteration	Henneberger and Browne (1988)
OK (340)	320	~1000 chloride springs discharge along east bank of Waikato River and on terraced surface of the Umukuri sinter over 2 km^2	Distributed flow in porous unwelded pyroclastic deposits), faults baffle reservoir at shallow depth (<50 m); intersection of topography and water table controls spring distribution	Bedded rhyolitic pyroclastic deposits	Breached ramp between major normal faults	0.38	14.5	Unknown	Lloyd (1972)
RK (300)	150	Strongest thermal activity on northern edge of Lake (a young hydrothermal eruption crater) and Parariki stream; total discharge of mixed chloride-sulfate water <10 kg/s	Flow through fractures dominate in the basement graywacke and overlying andesite lavas; distributed flow in rhyolitic volcanic rocks	Horizontally bedded volcanic deposits (rhyolitic) from surface to ~1,500 m depth, overlying ~1,000 m thick sequence of andesitic lavas, which are in unconformable contact with graywacke basement	Hydrothermal vents aligned on NE-SW trend, parallel to rift fabric	7.1	16.9	Sinter Flat contains ~2,500 kg Au + 2,500 kg Ag with As + Sb in silicieous muds formed from mixed acid sulfate-chloride springs	Weissberg (1969), Krupp and Seward (1987), Browne (1989), Reyes et al. (2003)
WM (325)	290	Choride springs restricted to SW part of a 16 km long line of volcanic vents formed 10 June, 1886; Frying Pan Lake hosts 5 subvents formed during 1917 hydrothermal eruption, discharges water (~55°C) at 100 to 120 kg/s	Volcanic craters formed during the 1886 eruption of Mount Tarawera and their intersection with the Haroharo caldera are important in near surface	Presumably bedded volcanic deposits which filled in SW corner of Haroharo caldera	Basalt fissure at caldera-rift intersection	7.9	115	Unknown	Keam (1981), Simmons et al. (1993, 1994), Bibby et al. 1995)
WT (610)	290	Chloride springs, silica sinter, mud pools, fumaroles + steaming ground within 10 Ωm contour; Champagne Pool = highest discharge ~10 kg/s; Waikite springs discharges on western edge of Waiotapu system: total area of thermal activity <0.5 km^2 along base of Paeroa Fault scarp; 3 chloride springs form bulk of deep fluid discharge of 7 kg/s	Weak focusing of flow through fractures in dense welded ignimbrites as indicated by narrow veins (<1 cm wide); distributed flow in porous unwelded pyroclastic deposits	Horizontally bedded volcanic pyroclastic deposits and lavas to >1 km thickness	Caldera boundary faults at southern edge of field, rift parallel normal faults bound NE edge of field	10.5	115	Champagne Pool contains 540 ppm Au + 750 ppm Ag in As-Sb-S–rich precipitates (2% As + 2% Sb); disseminated Au (<0.2 ppm) and Ag (<70 ppm) occur in altered rocks <500 m depth	Lloyd (1959), Hedenquist and Henley (1985, Hedenquist and Browne (1989), Hedenquist (1991), Giggenbach et al. (1994), Grindley et al. (1994), Pope et al. (2005)

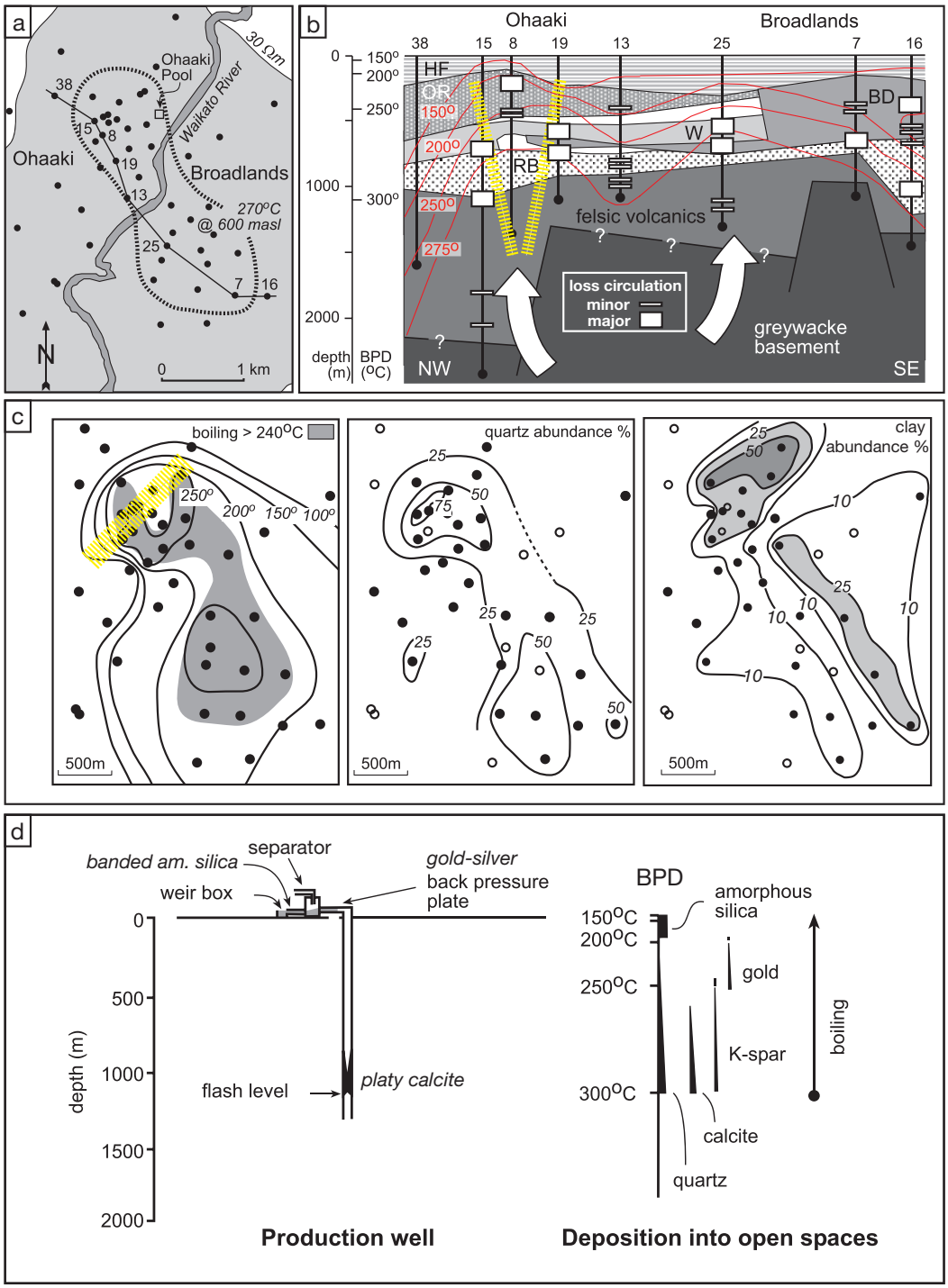

FIG. 3. Broadlands-Ohaaki geothermal system (after Simmons and Browne, 2000). (a). Plan view map showing well locations used to construct section line. (b). Cross section depicting circulation losses during drilling which represents localized zones of permeability (white rectangles), isotherms (red), flow paths (white arrows), and stratigraphy. Main aquifers: Rautawiri breccias (RB) and Waiora Formation (W). Aquicludes and aquitardes: Ohaaki Rhyolite (OR), Broadlands Dacite (BD), and Huka Falls Formation (HF). BPD scale (left) = boiling point for depth temperature curve. Yellow dashed lines = inferred position of Ohaaki fault zone. (c). Maps showing temperature gradients, quartz abundance, and distribution of clay minerals at 400 m depth. Filled circles represent drill core locations for data points; open circles represent drill locations lacking core. Yellow dashed line = Ohaaki fault. (d). Schematic diagram showing sites of mineral deposition in a production well. Gold and silver precipitate with chalcopyrite on the downstream side of the back-pressure plate. Colliform-crustiform banded amorphous silica deposits between the separator and the weir box, and platy calcite deposits downhole above the flash (boiling) level within the well. The distributions of minerals that deposit from boiling based on a numerical simulation are shown on right (BPD = boiling point for depth temperature); see Simmons and Browne (2000) for a detailed description of the simulation.

drill core have been supplanted by well production data and reservoir modeling, which suggest that bulk-rock permeabilities reach maximum values of 10^{-14} to 10^{-13} m^2 (e.g., Grant et al., 1982). Wells produce a mixture of steam and liquid at flow rates between 50 and 120 kg/s at 260° ± 20°C from feed zones mostly between 800 and 1,000 m depth (Fig. 3b). In its natural preexploitation condition, the overall flow rate for the system was only 100 kg/s.

Hydrothermal alteration is strongly zoned around the upflow zone, matching mineral patterns around epithermal orebodies (Simmons and Browne, 2000). The intensity of hydrothermal alteration diminishes outward from the center of the system, grading into fresh rocks on the periphery. Quartz, illite, K-feldspar (adularia), albite, chlorite, calcite, and pyrite are the primary hydrothermal minerals present in the deep central upflow zone at ≥250°C and >600 m depth. These minerals form through hydrothermal alteration of the volcanic host rocks by dilute, near-neutral pH chloride waters (Simmons and Browne, 2000). On the periphery of the upflow zone, illite, smectite, calcite, and siderite form through hydrolytic alteration in the presence of CO_2-rich steam-heated waters. The zone of maximum mineral deposition occurs in the shallow upflow zone and is defined by patterns of quartz abundance and K-feldspar occurrence, which appear influenced by the NE-striking Ohaaki fault; clay abundance, by contrast, is greatest on the shoulder of the upflow zone (Fig. 3c).

Gold and silver precipitate in three distinct environments (Simmons and Browne, 2000): (1) on back-pressure plates in production wells (Fig. 3d), (2) as low-grade disseminations in altered volcanic rocks, and (3) at the surface in the Ohaaki Pool. The flow conditions of geothermal wells are the most important in terms of understanding the formation of epithermal vein mineralization. The chloride waters feeding the wells are greatly undersaturated in gold and silver, but the combination of gas loss and cooling due to boiling result in quantitative precious metal deposition. Spectacular concentrations of precious metals (up to 5 wt % Au and 25 wt % Ag) precipitate with chalcopyrite on back-pressure plates due to sharp pressure-temperature gradients and boiling conditions (Brown, 1986). Lattice calcite and colloform-crustiform banded amorphous silica also deposit in wells, and both are distinctive features of quartz-adularia epithermal veins (e.g., Simmons et al., 2005). Widespread but low-grade disseminated precious metal mineralization (<1 ppm Au, <10 ppm Ag), associated with quartz-adularia-illite-calcite-pyrite–altered volcanic rocks at <500 m depth make up the second environment of metal deposition. Gold and silver transport and deposition resulted from the same rising chloride waters responsible for mineralization in the wells, but flow conditions contrast strongly, dominated by slow movement and tortuous pathways (Simmons and Browne, 2000). The third environment of metal depositions occurs at the surface in Ohaaki Pool where for a brief period in 1957, gold and silver deposited with Tl, Hg, As, Sb, and S (Weissberg, 1969). This mineralization is similar to that forming in Champagne Pool at Waiotapu and around Sinter Flat at Rotokawa, described below, and it forms by precious metal adsorption onto As and Sb sulfur colloids (Renders and Seward, 1989). This hot-spring environment, however, does not appear to be significant in terms of total metal deposited.

Waiotapu

Waiotapu (Figs. 2, 4) has high heat flow, extends over a large area, and is notable for precipitation of gold and silver in Champagne Pool (a 700 yr old hydrothermal eruption vent; Hedenquist and Henley, 1985). The 10 Ωm (500 m electrode spacing) resistivity contour delimits the geothermal field and encompasses a 10.5 km^2 region of high natural heat flow (610 MW_{th}) centered on the Waiotapu Basin (Bibby et al., 1995).

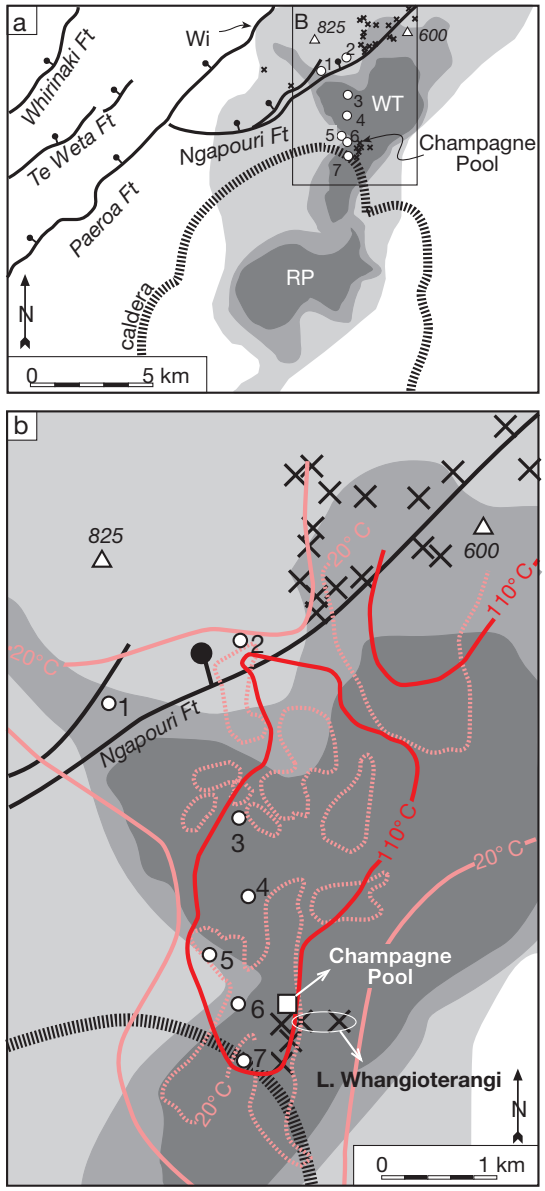

FIG. 4. (a). Map of Waiotapu (WT), Waikite (Wi), and Reporoa (Re) geothermal systems showing inferred caldera boundary (black dashed line), major faults (tick on downthrown side), and topographic highs (white triangles with elevation in meters above sea level). Drill holes are shown by white circles and are numbered 1 to 7. X = locations of hydrothermal eruptions. Shading indicates shallow resistivity (Bibby et al., 1995): dark gray = <10 Ωm, mid gray =10 Ωm, light gray =10 to 30 Ωm. (b). Detail map of Waiotapu geothermal field. Isotherms at a depth of 30 m are shown for temperatures of 110° and 20°C (solid red and pink line, respectively), and the 20°C isotherm is shown at 1 m depth (dashed pink line; Thompson, 1963; Hedenquist, 1991).

However, Waiotapu is the middle of three closely spaced geothermal systems, including Waimangu to the north and Reporoa to the south. The 30 Ωm resistivity contour (500 m electrode spacing), which encircles all three systems, covers 115 km² (Bibby et al., 1995, 1998) and likely marks the extent of contiguous hydrothermal alteration at <500 m depth.

Surface thermal activity comprises fumaroles, acid sulfate mud pools, and near-neutral pH chloride springs (most at near-boiling temperatures), with >100 kg/s of hot water discharge (Hedenquist, 1991; Giggenbach et al., 1994). Two dacite domes (600–825 m asl) bound the thermal area in the north, and the upthrown, footwall block (~500 m asl) of the Paeroa fault (>600 m of offset) bounds the field in the west. The trace of this fault transects the western edge of the 30 Ωm resistivity boundary and coincides with localized discharge (~75 kg/s) of chloride-bicarbonate springs at Waikite. Waiotapu is dissected by ring faults associated with the northern margin of the Reporoa caldera (Nairn et al., 1994), which along with the NE-striking Ngapouri fault, host numerous hydrothermal eruption vents (Hedenquist and Henley, 1985; Nairn et al., 2005).

The subsurface hydrology is deduced from seven drill holes (WT 1-7, Fig. 4) penetrating to depths of 500 to 1,100 m and spring chemistry (Hedenquist and Browne, 1989; Hedenquist, 1991; Giggenbach et al., 1994; Grindley et al., 1994; Wood, 1994; Wilson et al., 2010a). The stratigraphy comprises nearly flat-lying felsic pyroclastic deposits and reworked equivalents, andesite and dacite lava flows, and lacustrine sedimentary rocks, which form alternating aquifers and aquicludes. Deep fluids ascend along temperature and pressure gradients that are close to boiling in the vicinity of Champagne Pool and near WT-4; a maximum temperature of 295°C was measured at 1,000 m in WT-7. In the very near surface, the pattern of 1 and 30 m deep 20°C isotherms demonstrates that hydrothermal flow subdivides into narrow vertical columns as it ascends (Hedenquist, 1991: Fig. 4b). The 30 m deep 20°C isotherm is similar in extent and location to the region of surface thermal activity as demarked by the 10 Ωm resistivity contour. In contrast, the 1-m-deep anomalies are localized, they are elongate in a NE or NW direction, and they encircle surface thermal features. About half of the total mass of hot chloride water is deflected southward through shallow aquifers, with the remainder discharging through to the surface (Hedenquist, 1991).

Champagne Pool is a hydrothermal eruption vent (~60 m deep, ~60 m diam) that is one of more than 20 hydrothermal eruption vents in the Waiotapu area. Most vents are filled with cold lakes, and they occur along the Ngapouri fault in the northern part of the field. There are at least six hydrothermal eruption vents in the vicinity of Champagne Pool, and all are associated with hot-spring discharge. Inferred eruption depths range from <170 to 350 m beneath the surface (Hedenquist and Henley, 1985). These vents lie less than 500 m outside the structural boundary of the Reporoa caldera (Fig. 4). Three ^{14}C age dates on hydrothermal eruption deposits and stratigraphic relationships suggest that the eruptions took place around 700 years ago, synchronous with rhyolite eruptions at Mount Tarawera, ~15 km northeast of Waiotapu (Fig. 2; Lloyd, 1959; Grant-Taylor and Rafter, 1971; Hedenquist and Henley, 1985; Nairn et al., 2005). Bright orange, sulfur-rich precipitates accumulating in Champagne Pool contain up to 12 wt % As, 46 wt % Sb, 540 ppm Au, 745 ppm Ag, and significant Tl and Hg (Pope et al., 2005). Deeply derived water with the highest chloride concentration (~2,000 ppm Cl) overflows the pool at ~10 kg/s. The temperature of the water is uniform at 74°C due to rapid convection in the pool (Hedenquist and Henley, 1985). A relatively high aqueous CO_2 concentration is indicated by the nucleation and exsolution of gas bubbles around the edge of the pool. This maintains a weakly acidic pH ~5 that stabilizes precipitation of the amorphous arsenic and antimony sulfur colloids, which are highly efficient at adsorbing Au and Ag from solution (Hedenquist and Henley, 1985; Renders and Seward, 1989; Pope et al., 2005).

Rotokawa

Rotokawa is located in the southeastern part of central Taupo Volcanic Zone in gentle terrain (300–400 m asl) ~5 km northeast of Wairakei (Figs. 2, 5). Precious metals precipitate in both geothermal wells and in hot springs around Lake Rotokawa in depositional environments resembling those described above for Broadlands-Ohaaki and Waiotapu, due to the relatively high concentration of aqueous H_2S in deep fluid (Krupp and Seward, 1987; Reyes et al., 2003; Simmons and Brown, 2007). The subsurface hydrology is interpreted from seven wells drilled before 1990 (the results of more recent drilling have yet to be published). Geothermal wells penetrate to >2.7 km where temperatures up to 335°C were measured (Browne, 1989). Flat-lying rhyolitic lavas and pyroclastic deposits extend from the surface to ~1,500 m depth and overlie a sequence of andesite lava flows ~1,000 m thick (Brown et al., 1992). Basement rocks consist of block-faulted graywacke. Permeability in the graywacke and andesite is controlled by near-vertical faults and fractures that focus

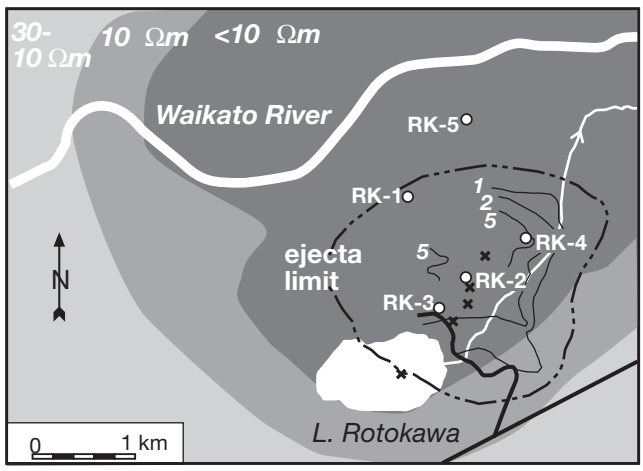

FIG. 5. Map of southern part of the Rotokawa geothermal system showing resistivity contours: dark gray = <10 Ωm, mid gray =10 Ωm, light gray =10 to 30 Ωm. Drill holes are shown by white circles and are numbered RK-1 to RK-5. X = locations of hydrothermal eruption vents, one of which is centered on Lake Rotokawa (white polygon). Ejecta isopachs (m) and ejecta limit (dashed black line) are shown for largest hydrothermal eruption described at this site (Collar and Browne, 1985).The Waikato River is shown by a thick white line; Parariki stream draining Lake Rotokawa shown by thin white line; roads shown by black lines.

upflow. Surface thermal activity, comprising steaming ground, fumaroles, and springs, is concentrated in an area (~1.2 km²) extending northeast from the edge of Lake Rotokawa. About 2,500 kg of gold and 2,500 kg of silver were deposited with As and Sb in siliceous muds of Sinter Flat (100 × 200 m) on the north shore of the lake from mixed acid sulfate-chloride springs (pH = 4–5, T = 70°–90°C) discharging at ~6 kg/s (Weissberg, 1969; Krupp and Seward, 1987).

Relevant to this study are the occurrences of hydrothermal eruption vents, which appear to delineate a NE-striking structure. Breccia deposits from at least eight hydrothermal eruptions (dating back to 22,000 years) cover the southern part of the field and result from some of the largest hydrothermal eruptions known in geothermal environments globally (Collar, 1985; Collar and Browne, 1985; Browne and Lawless, 2001). The largest eruption, ~6,000 years ago, is one of three sourced from Lake Rotokawa and produced deposits that cover an area of about 15 km²; the youngest eruption known occurred ca. 3,700 years ago. The vent locations of hydrothermal eruptions are deduced from isopach thicknesses of deposits and the distribution of large clasts (Collar, 1985). The vents align on a northeasterly trend, revealing the likely trace of a fault and a zone of elevated fluid flow extending >1 km along strike. Comparison of breccia clast lithologic units with the stratigraphy known from drill cores suggests that focal depths for some of the eruptions exceeded a depth of 450 m (Collar, 1985; Collar and Browne, 1985).

Waimangu

Waimangu is located along the southern margin of Okataina Volcanic Center, ~10 km north of Waiotapu (Figs. 2, 6). The hot-water discharge of Frying Pan Lake (100–120 kg/s), which occupies the western part of the Echo crater, is the highest for a single thermal feature anywhere in the

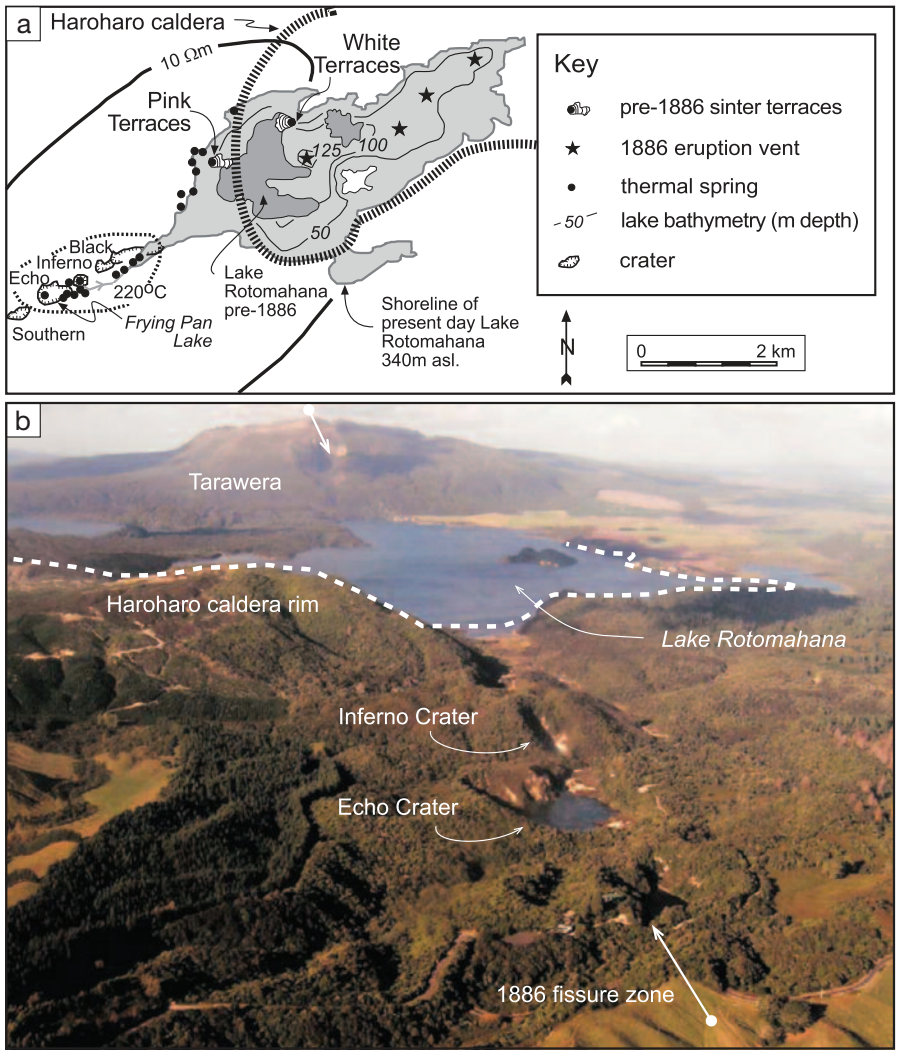

FIG. 6. (a). Map of Waimangu geothermal system showing position of hot springs (black circles), the volcanic craters formed in the 1886 Tarawera basalt eruption (craters labeled), present and pre-1886 Lake Rotomahana, the 10 Ωm resistivity contour (solid black line), position of the Haroharo caldera boundary (dashed black line), and the 220°C isotherm based on aqueous Na/K ratios (Keam, 1981; Simmons et al., 1993). (b). Oblique aerial view of the Waimangu geothermal field looking northeast. Major features are labeled. The 1886 eruptive fissure zone is shown by paired arrows and extends beyond the prominent chasm visible on the flanks of Mount Tarawera.

Taupo Volcanic Zone, with a flow rate and power output similar to a geothermal production well.

The 10 Ωm (500 m electrode spacing) resistivity boundary outlines the extent of the system and straddles the southern margin of the Haroharo caldera. Surface thermal features are located near the intersection of the caldera structure and the line of volcanic craters that formed the 1886 Tarawera rift eruption (Keam, 1981; Simmons et al., 1993). Because geothermal wells have not been drilled here, the subsurface hydrology is interpreted from the occurrences of springs and their water compositions (Simmons et al., 1994). Near-neutral pH chloride springs (85°–100°C) are confined to the west shore of Lake Rotomahana and the Waimangu valley (Fig. 6), which incises a plateau composed of young felsic pyroclastic deposits and lavas. Low-discharge fumaroles and steaming ground occur in the high ground between the Echo, Inferno, and Black craters. Spring-water compositions have Na/K values that indicate deep equilibration temperatures between 240° and 280°C (Simmons et al., 1994).

The vents that feed the thermal discharge of Frying Pan Lake formed 1–3 April, 1917, during a series of hydrothermal eruptions lasting 3 days. However, the relevant history of volcanic and geothermal activity preceding formation of Frying Pan Lake dates back to 1886 when the locus of surface activity was concentrated around the small, shallow ancestral Lake Rotomahana, which was home to large silica sinter deposits known as the Pink and White Terraces (Fig. 6a). These terraces were destroyed by the short but powerful 10 June, 1886, dike intrusion and eruption of basalt from Mount Tarawera (Figs. 2, 6b; Nairn and Cole, 1981). The resulting volcanic craters produced strong vertical permeability allowing cold-water egress that suppressed surface thermal activity for ~5 years. The gradual infilling of the modern Lake Rotomahana caused hot water discharge in and around the Inferno and Echo craters, starting in the early 1890s. From 1900 to 1917, there were two important episodes of explosive outbursts. The Waimangu geyser with cyclical hydrothermal eruptions played between 1901 and 1904 in the eastern part of the Echo crater, jetting hot water, steam, and rock material >300 m high. In 1917, large hydrothermal eruptions forming Frying Pan Lake broke out from the western part of the Echo crater. The eruptions produced five funnel-shaped subvents (each ~10 m diam) through which boiling hot water has been discharging through to the present (Keam, 1981). Volcanic context, high mass flux of thermal water, and the history of hydrothermal eruptions and geysering suggest that the subsurface permeability structure and fluid flow through the epithermal environment of the system is strongly affected by a pipelike vertical structure underlying the Echo crater plus adjustment to new shallow pressure-temperature gradients in the aftermath of the 1886 eruption (Simmons et al., 1993).

Te Kopia and Orakeikorako

Te Kopia and Orakeikorako are located at the southwestern tip of the Paeroa fault. These are the only geothermal fields that provide good surface exposure of steeply dipping normal faults (Fig. 7). Although Te Kopia and Orakeikorako are separated by ~5 km, there is considerable evidence for past hydrothermal activity between the two, and it is possible they were once part of a single large system (Clark and Browne, 1998; Fig. 7a).

The Paeroa fault extends for ~25 km in a NE-SW direction and forms a scarp rising 500 m above the valley floor. It exposes dense, welded pyroclastic flow deposits that were emplaced ~340,000 years ago (Grindley et al., 1994; Houghton et al., 1995) and tilted eastward <10° by normal fault displacement. Within the Te Kopia area, the fault comprises a zone of parallel structures that progressively step down toward the valley (Fig. 7a). Southwest of Te Kopia, the Paeroa fault bifurcates into a series of subparallel segments (Lloyd, 1972), in the ramp between the uplifted Paeroa block to the northeast and the Whakaheke block, which is offset to the west and south. Orakeikorako is located in a topographic low between these two major fault blocks.

Te Kopia straddles the Paeroa fault and thermal activity has evolved in response to fault displacement and uplift lasting more than 100,000 years (Bignall and Browne, 1994). Surface expression covers an area of about 3 km², and most of it is concentrated in the footwall block, characterized by widespread steaming ground and strong fumaroles. Murphy's springs represent low thermal discharge (<1 kg/s total mass flux) of mixed bicarbonate-chloride waters in the north part of the field. Three hydrothermal eruption craters 100 to 200 m in diameter occur along the base of the fault scarp and are filled by shallow pools of acid sulfate water. Blocks of silica sinter dated at >1,800 years old (Martin et al., 2000) indicate that near-neutral pH alkali chloride waters discharged here in the past, but a drop in relative position of the water table, perhaps in association with fault displacement, has resulted in overprinting by steam-heated acid-sulfate alteration (Bignall et al., 2004).

Surface thermal activity at Orakeikorako presently encompasses an area of less than 2 km² and occurs where splays that structurally link the Paeroa block to the northeast and the Whakaheke block to the southwest cross the Waikato River (Fig. 7b). The stratigraphy comprises a sequence of flat-lying tuffs and reworked equivalents, along with minor basalt scoria deposits (Lloyd, 1972; Bignall, 1991). Four wells drilled in the 1960s outside the area of hot-spring activity had poor production but a maximum temperature of 265°C was encountered at about 1,400 m depth. Most thermal springs discharge dilute chloride or mixed chloride-bicarbonate waters of slightly alkaline pH. Before 1961, approximately 1,100 springs issued along the banks of the Waikato River, but impoundment of the river by the Ohakuri dam in 1961 flooded about 70% of these, including many spectacular geysers (Lloyd, 1972). The concentration of hot springs along the banks of the Waikato River in the western and southern parts of the field suggests that the intersection of topography and the water table are the main influence on their occurrence and distribution (Fig. 7b). However, vertical differences (~5 m) in the water table occur across fault blocks and indicate compartmentalization of the shallow hydrology (<50 m depth) where faults act as baffles rather than conduits for fluid flow (Rowland and Sibson, 2004).

Ohakuri

Hydrothermal activity at Ohakuri (Figs. 2, 8), which ended more than 42,000 years ago, produced subeconomic

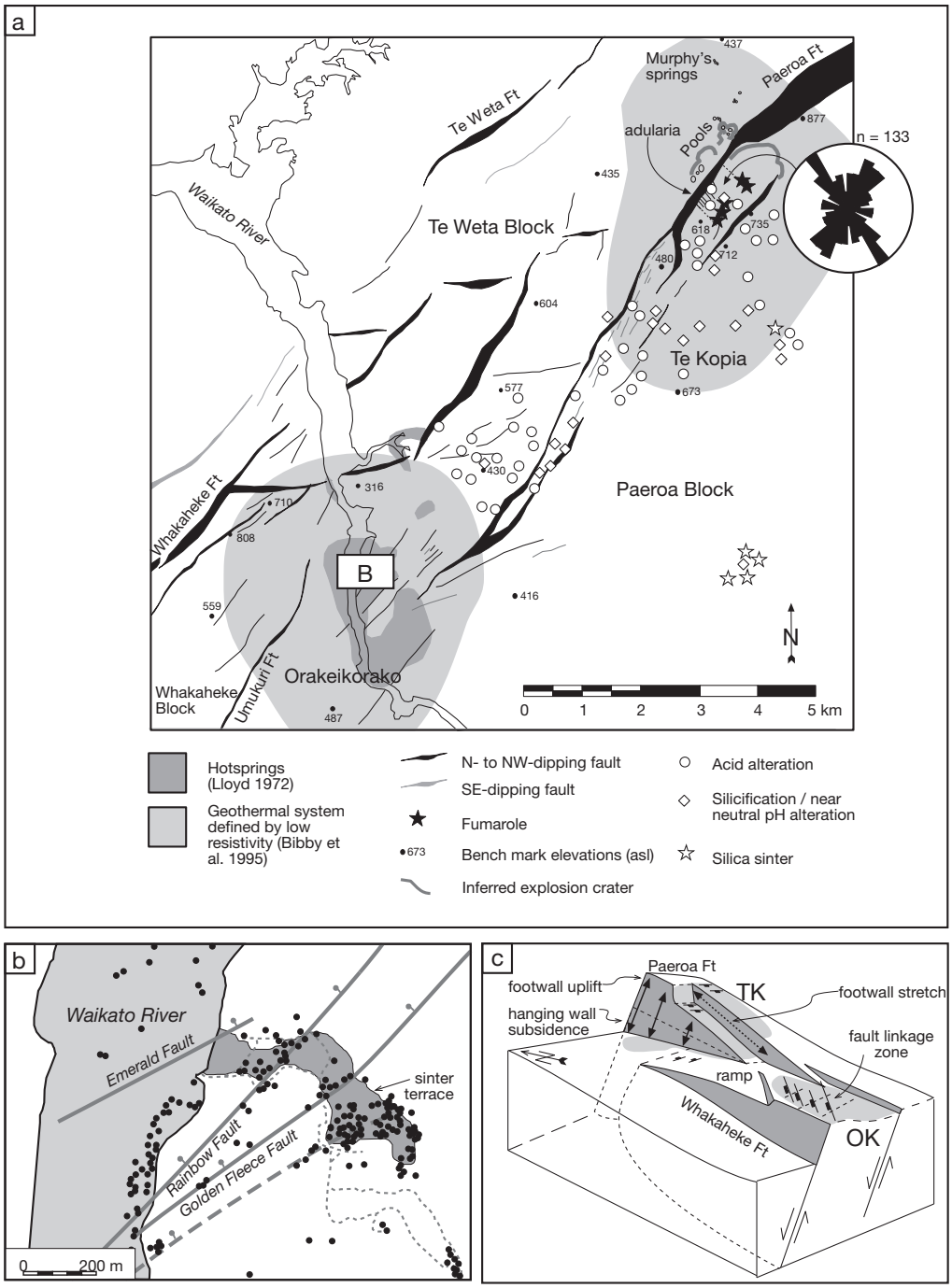

FIG. 7. (a). Structural setting of Te Kopia and Orakeikorako geothermal systems, showing location of detail map in (b) of the locations of hot springs in the central part of Orakeikorako (Lloyd, 1972). The main geothermal areas are delimited by the 30 Ωm resistivity contour (Bibby et al., 1995). Sites of hydrothermal alteration are classified as acid alteration consisting of kaolinite and alunite, silicification, and/or near-neutral pH alteration consisting of quartz with or without illite, smectite and adularia, and silica sinter which deposited from formerly active, near-neutral pH hot springs (Clark and Browne, 1998). Rose diagram shows the orientation of steeply dipping quartz veins in the footwall to the Paeroa Fault (Rowland and Sibson, 2001). Some veins strike NE and parallel the Paeroa fault, and other conjugate sets strike NW and form resistant ridges perpendicular to the scarp (indicated by short parallel lines). Bench mark elevations shown in meters above sea level (asl). The width of the fault line symbol represents the throw on the scarp. (b). Map showing the distribution of hot springs (black circles) at Orakeikorako in relationship to the Waikato River, small offset (<5 m) normal faults, and silica sinter (dark gray polygon). Springs in river were flooded in 1960 by dam impoundment. Walking tracks shown by dashed gray lines. (c). Schematic block diagram of the step-over area between the Paeroa-Whakaheke Faults, showing a region of intense fracturing near the upper ramp (after Crider and Pollard, 1998), and strike-parallel extension in the footwall to the Paeroa Fault (Ferrill and Morris, 2001). Locations of Te Kopia and Orakeikorako geothermal fields (light gray) coincide with locally enhanced fault and extension fracture density related to growth and linkage of the two first-order faults.

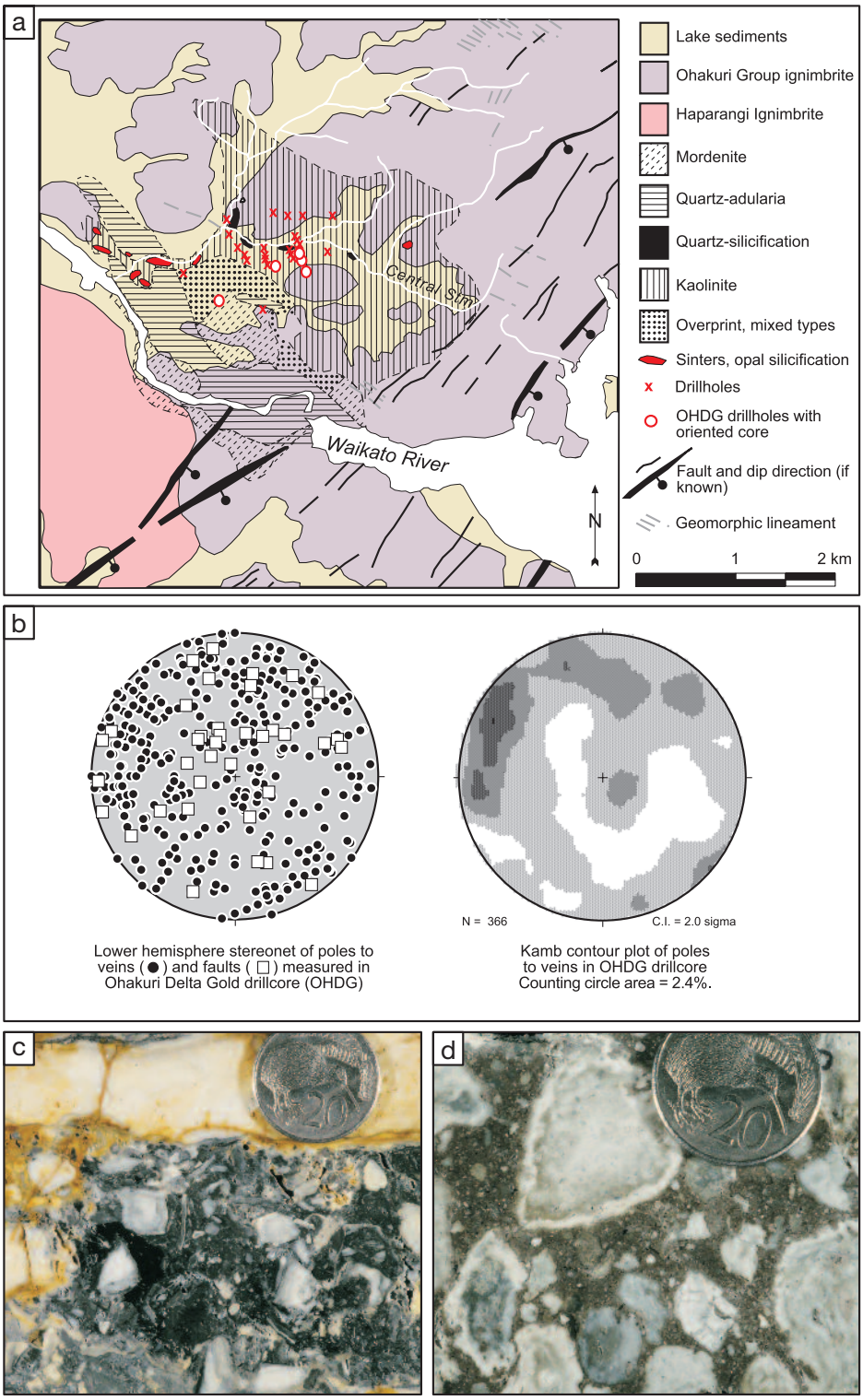

FIG. 8. (a). Map of Ohakuri showing distribution of hydrothermal alteration (mordenite, quartz-adularia, quartz silicification, and kaolinite; Henneberger and Browne, 1988), inferred faults (the width of the fault line symbol represents the throw), drill holes with oriented core (red circles with white fill), and other drill holes (red x). (b). Lower hemisphere equal area stereonets showing uncontoured and contoured poles to faults and veins measured in oriented core in OHDG drill holes. (c). Photograph of outcrop sample from Ohakuri showing quartz vein with two main phases of infill comprising early light quartz and later dark quartz + pyrite; note that the gold grade is evenly distributed at ~2 g/t Au. (d). Photograph of core sample from Ohakuri, showing pumiceous host rock completely and pervasively altered to quartz and adularia, with subeconomic disseminated gold mineralization (~0.1 g/t Au). This material is representative of the lithology, alteration, and mineralization throughout the prospect at <120 m depth. Coin in (c) and (d) is 30 mm across.

disseminated precious metal mineralization containing >2 million oz (Moz) gold (Henneberger and Browne, 1988; Grieve et al., 2006). Mineralization is contained within quartz-adularia–altered pyroclastic deposits, which crop out and extend to 200 m depth. The paleosurface of the deposit is preserved in the northern part of the area as reflected in isolated outcrops of silica sinter, hydrothermal eruption breccias, and widespread alunite-kaolinite alteration that formed from steam-heated acid sulfate waters. The blanket-like zone of precious metal mineralization underlies an area >10 km^2, and it was extensively explored in the late 1980s and early 1990s, with more than 40 diamond drill holes. Many of these holes were sited near Central Stream, an inferred late-stage E-W–striking upflow zone, in order to test the existence of a feeder structure at depth (Fig. 8a). Despite encouraging intercepts (>1 g/t Au), most gold mineralization is low grade (0.1–1.0 g/t Au) and disseminated, and associated quartz-pyrite veins are widely spaced, anastomosing, short (<5 m) and narrow (<1 cm; Henneberger and Browne, 1988). Vein orientations are only weakly clustered, with a slight predominance of steep NE-striking structures (Fig. 8b). One of the widest known epithermal veins in Ohakuri is 10 cm across (Fig. 8c) and contains ~2 g/t Au; quartz pseudomorphs of platy calcite occur locally indicating boiling conditions (e.g., Simmons and Christenson, 1994).

Judging from rock textures (Fig. 8d), the ignimbrite that hosts the intense quartz-adularia-gold mineralization originally comprised porous, unwelded pumice breccia that was permeable and allowed distributed, intergranular fluid flow. Alteration and silicification filled most pore space, creating hard and dense rock in which weak vein stockworks subsequently developed (Henneberger and Browne, 1988). Thus, the character of permeability transformed with time, such that distributed hydrothermal flow through porous media became focused within fracture networks.

Factors Affecting Hydrothermal Fluid Flow

Hydrothermal fluid-flow paths are transient. At large spatial scale they are controlled by the supply of deep magmatic heat, which makes hot water buoyant, forming hydrothermal plumes on which geothermal systems are centered. This type of flow can be described using Darcy's law, which quantifies the effect of a pressure differential on fluid flow through porous media. In the Taupo Volcanic Zone, where depth to the base of the convection zone is 6 to 8 km, the pressure difference between hot and cold hydrostatic head of ~10 MPa is the main control on large-scale fluid flow (e.g., Rowland and Sibson, 2004; Grant and Bixley, 2011). By contrast, physiographic relief is generally less than 200 m giving differential pressures ≤2 MPa, which is only sufficient for creating shallow outflow zones (e.g., Bibby et al., 1995). The variation in dynamic viscosity is also small (Manning and Ingebritsen, 1999; Cox et al., 2001), and this makes permeability the critical variable in dictating the magnitude of fluid flow. As indicated in Figure 9, permeability varies over several orders of magnitude depending on rock type, but the minimum bulk permeability required for convection is 10^{-16} m^2, giving rise to a simple overall plume structure (Elder, 1981; Henley and Ellis, 1983; Cathles et al., 1997). The actual permeability structure for any volume of rock is far more complex than captured in estimates of bulk permeability. Because rocks, faults, and fractures are subject to transformation by seismicity, and mineral deposition and dissolution, flow paths continuously evolve both gradually and spasmodically. Moreover, at any particular time, the total volume of rock directly involved with the transmission of fluid is very small compared to the overall volume of rock which hosts the flow network, as appears evident for Ohaaki (Fig. 3b) and other geothermal systems (Donaldson and Grant, 1981; Elder, 1981; Grant et al., 1982; Hanano, 2004). High-flux conduits only seem to occur under exceptional situations. Here we focus our attention on

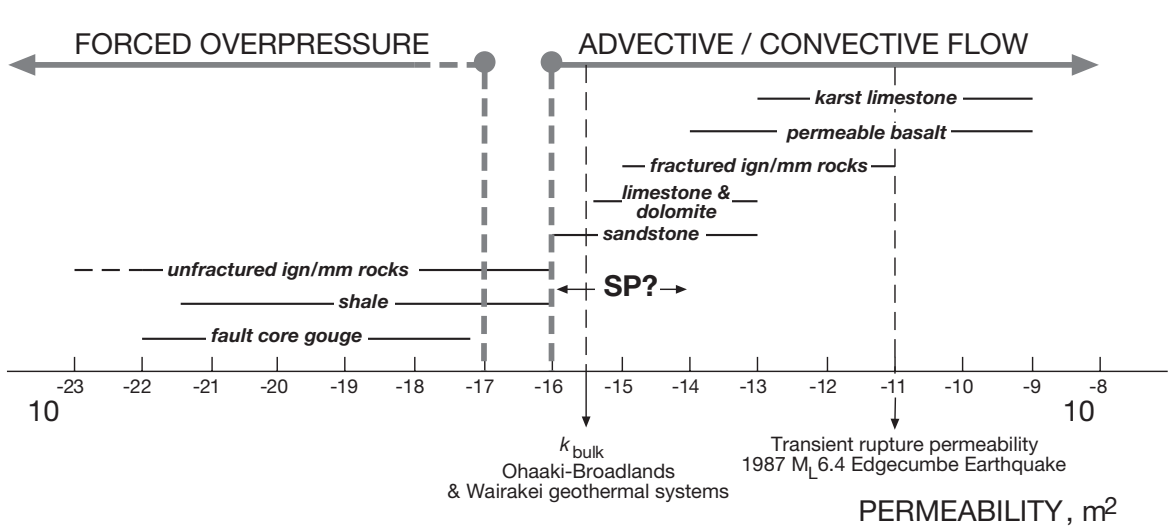

FIG. 9. Critical bounds to bulk permeability allowing hydrothermal convection (Cathles et al., 1997) and development of forced overpressures (Neuzil, 1995) in relationship to permeability values for consolidated crustal rocks (Brace, 1980), and permeabilities of fault gouge from the core of large displacement faults (Wibberley and Shimamoto, 2003). SP = estimates of seismogenic permeability from migration of microearthquakes (Talwani and Acree, 1984). Bulk permeability inferred for Broadlands-Ohaaki is shown (McNabb, 1975), as is the transient permeability inferred for the 1987 Edgecumbe earthquake.

the roles that lithology, alteration and mineralization, and faulting play in controlling fluid flow and forming these conduits.

Crustal heterogeneity

The heterogeneous assemblage of lithologic units present within the Taupo Volcanic Zone results in large lateral and vertical variations in permeability. The stratified Quaternary volcanic sequence approximates a layered medium, which induces a strong contrast between layer parallel and layer perpendicular permeability, with the latter controlled by the low-permeability layers (Manning and Ingebritsen, 1999). A vertical to horizontal permeability ratio of 1:40 is possibly representative of the volcanic stratigraphy down to 3 km depth based on the results of numerical reservoir models (e.g., Mannington et al., 2004). Despite the abundance of granular layers conducive to diffuse flow within the Quaternary volcanic sequence, macroscopic faults and fractures must comprise an important component of crustal-scale permeability for two reasons: (1) intergranular porosity, and thus permeability, decreases with depth in granular materials (pyroclastic and sedimentary rocks) as a consequence of diagenetic processes (Björlykke, 1997; Stimac et al., 2004, 2008), and (2) metasedimentary rocks, if present within the convective regime (e.g., Broadlands-Ohaaki), have insufficient permeability to sustain geothermal production, except where drilling has intercepted hydraulically conductive faults and fractures (Wood et al., 2001). Although the lithologic and hydraulic characteristics of basement rocks are poorly known for most of the central Taupo Volcanic Zone, the density structure, based on gravity and seismic data, is consistent with the presence of graywacke metasedimentary rocks, andesitic lavas and/or welded or silicified ignimbrites (Stern, 1986). Convective flow through any of these rock types requires fault and/or fracture-controlled permeability (Rowland and Sibson, 2004).

The quasiplastic regime in the vicinity of deep (>6 km for the Taupo Volcanic Zone) intruding magmas, and where heat transfer by conduction prevails, is generally considered impermeable in terms of advective fluid flow unless deformation processes enhance permeability via fracturing, microfracturing, or creep-induced cavitation (Cox et al., 2001; Cox, 2005, Micklethwaite et al., 2010). In addition to episodic rupturing of the brittle-ductile transition in association with large earthquakes, shear zones and creeping faults are likely to be an important means of channeling liquids from deep sources to the base of the seismogenic zone (Cox et al., 2001). Seismogenic processes thus may be of particular importance near the base of high-temperature convection cells, allowing entrainment of magmatic fluids into the meteoric convection regime.

Hydrothermal alteration and mineral deposition

Steep physical and chemical gradients in the top 1 to 2 km of the geothermal system drive mineral dissolution, transformation, and precipitation. Permeability, porosity, and rock strength are continually modified as a function of time and space (e.g., Browne and Ellis, 1970; Hedenquist and Browne, 1989; Simmons and Browne, 2000). Despite their inherent variability, once a geothermal system becomes long-lived (>50 ky), three first-order effects can be recognized. First, clay-rich alteration forms in shallow steam-heated aquifers and on the periphery of the upflow zone (e.g., Hedenquist and Browne, 1989; Hedenquist, 1990; Simmons and Browne, 2000). This type of alteration likely reduces permeability as well as rock strength by increasing the proportion of clay minerals that replace volcanic glass and feldspars. Second, silicification and K metasomatism due to deposition of quartz and adularia from rising and cooling chloride waters reduce porosity and permeability but increase rock strength (e.g., Ohakuri; Henneberger and Browne, 1988). This effect is most pronounced at <500 m depth in the central upflow zone of a system, as demonstrated at Broadlands-Ohaaki (Fig. 3c; Simmons and Browne, 2000), where it enhances the development of fault-fracture–related permeability. Third, mineral deposition can line and therefore isolate high-permeability pathways from incursion of fluid from the surrounding country rock.

In the upflow zone, fracture permeability will become increasingly important with time, a consequence of the gradual destruction of intergranular permeability by pervasive silicification and mineral deposition. Accordingly, some fluctuations in pore fluid pressure may be expected. Within explored Taupo Volcanic Zone geothermal systems, measurements of back flow from overpressured zones during drilling (locally known as "well kicks") indicate that fluid pressure generally does not exceed 20% above cold hydrostatic values (Browne and Lawless, 2001), at least during interseismic periods. Thus, despite ongoing hydrothermal mineral deposition within the hydrothermal upflow zones, fluid-flow paths at <2.5 km depth appear to be maintained at near-hydrostatic pressure conditions, with rare excursions to superhydrostatic pressure due to mineral sealing (Simmons et al., 2007). Because significant overpressuring seems to occur rarely, the rock mass may be critically primed for failure so that small increases in fluid pressure immediately trigger microseismic events (cf. Townend and Zoback, 2000). Two lines of evidence support this notion. First, at Rotokawa, microseismicity within the upflow zone is induced by the reinjection of waste water (e.g., Heise et al., 2008). Second, recent analyses of earthquakes ($0.4 < M_L < 5$) occurring from 1984 to 2004 in and around the Rotorua and Kawerau geothermal systems (Fig. 2) reveal seismogenic structures in the midcrust whose positions and geometries are consistent with previously published fault mechanisms and known near-surface faults (Clarke et al., 2009). A mechanical treatment of this point is presented in the next section.

At the base of the geothermal system permeability is also influenced by steep physical and chemical gradients, which cause mineral dissolution, transformation, and precipitation (e.g., White and Mroczec, 1998). Because fault-fracture networks control deep fluid flow, episodic, and localized fluctuations in pore fluid pressure resulting from mineral sealing (and dissolution) likely operate at short timescales of 1 to 1,000 years at this structural level. Brittle failure induced by increases in pore fluid pressure may explain the common occurrence of seismic swarm activity toward the base of the seismogenic zone (Sherburn et al., 2003). These short-term local-scale (swarms typically affect crustal volumes of only a few 10s to 100s m^3), fluctuations may be critical in maintaining the stability of geothermal flow at longer spatial and temporal scales.

Brittle deformation and conditions for development of high-flux fluid conduits

Fluid flow and transport behavior is governed overwhelmingly by the distribution of fracture conductivity within the upper crust. However, characterizing the three-dimensional geometry of fracture networks, and defining a quantifiable connection between geometrical and hydraulic connectivity, is a major challenge to understanding flow in fractured geologic media (Berkowitz, 2002). Here, we take a qualitative approach to illuminate some of the factors we think are important in the development of high-flux conduits. These include macroscopic mode of brittle failure, lithology and stratigraphy, the seismic cycle, and degree of sealing through hydrothermal cementation (Sibson, 2000). Brittle structures rarely form in isolation and their cumulative hydrologic effect additionally exerts an important control on permeability heterogeneity and anisotropy (e.g., Rowland and Sibson, 2004).

Three macroscopic modes of brittle failure are possible: shear failure (faulting), hybrid extensional-shear failure, and extensional failure (Sibson, 1998). Extensional failure involves the generation of dilational fractures perpendicular to the orientation of the least principal stress, σ_3. Shear failure involves displacement parallel to the fracture surface, and hybrid extensional-shear failure involves components of shear and dilation. The mode of brittle failure depends upon pore fluid pressure, P_f, differential stress defined by the difference between the greatest and least principal stresses (σ_1–σ_3), and tensile strength, T, of the deforming rock volume, which is modulated by hydrothermal alteration and mineral deposition. In tectonically active regimes that promote fluid flow, P_f, (σ_1–σ_3) and T vary temporally and spatially. The effect on failure mode can be usefully illustrated in pore fluid factor and differential stress space, where the pore fluid factor, λ_v, is the ratio between fluid pressure and overburden σ_v (Cox, 2010). Relevant failure criteria and assumptions for this analysis are listed in Table 2.

Figure 10a-c shows the effect of varying the tensile strength on conditions for permeability enhancement during intact rock failure at 4,000, 2,000, and 200 m depths within the Taupo Volcanic Zone. Composite failure curves for intact rock of tensile strengths, T = 1, 5, 10, 20 MPa, are constructed assuming a representative coefficient of internal friction, μ = 0.75, and densities of 2,650, 2,500, and 2,200 kg/m^3 for each depth level, respectively. These tensile strengths represent the range of rock competencies encountered in drilled parts of Taupo Volcanic Zone geothermal systems. Most of the pyroclastic material and reworked sediments are very weak (<<5 MPa). Rhyolites may be a little stronger (<10 MPa), and andesites and graywackes are expected to have tensile strengths somewhere between 10 to 20 MPa (Rowland and Sibson, 2004). Also shown is the failure envelope for reshear of an optimally oriented and cohesionless fault with μ_s = 0.75. Cold hydrostatic and lithostatic conditions are annotated on the plots for reference together with the expected limiting condition for overpressures within Taupo Volcanic Zone geothermal systems (λ_v < 20% above cold hydrostatic pressure). These plots illustrate several important points: (1) with decreasing depth, normal faults steepen into the orientation of subvertical extension fractures; (2) the mode of brittle failure is extremely sensitive to variations in pore fluid pressure and tensile strength within the epithermal environment (z <2,000 m); (3) shear failure predominates at greater depth for most Taupo Volcanic Zone rock types and expected fluctuations in pore fluid pressure; and (4) the presence of a throughgoing cohesionless fault optimally oriented for reactivation precludes all other forms of brittle failure in intact rock (Sibson, 1998; Cox, 2010).

Assuming our tensile strength values are appropriate, much of the stratigraphy is too weak to favor the development of open fractures except over short vertical extent (as controlled by the thickness of competent rock) or near the surface. Open fractures and mixed-mode fault-fracture meshes are possible where intercalated andesites, rhyolites, or strongly welded ignimbrites occur within the stratigraphy, or where silicification has made the rocks more susceptible to pure extension or extensional-shear fracturing (e.g., Ohakuri: Henneberger and Browne, 1988). Grindley and Browne (1976) provided the best description of mixed-mode fault-fracture meshes within the Taupo Volcanic Zone based on drill hole data. They describe circulation losses during drilling at depths consistent with the positions of inferred faults (Fig. 3b). At many of

TABLE 2. Failure Criteria in Pore Fluid Factor-Differential Stress Space (Cox, 2010)

Macroscopic mode of brittle failure	Failure criteria	Assumptions	Limitations
Brittle shear failure on optimally oriented faults in intact rock	Coulomb criterion $\tau = C + \mu(\sigma_n - P_f)$, where τ = shear stress, C = cohesive strength, μ = coefficient of friction in an isotropic rock mass, σ_n = normal stress, P_f = pore fluid pressure; for a fault inclined θ_{opt} to σ_1 $\lambda_v = [4C - \sigma_1 + 4\sigma_3]/3\sigma_v$, where σ_v = overburden, pore fluid factor $\lambda_v = P_f/\sigma_v$ and $\theta_{opt} = \frac{1}{2}\tan^{-1}\mu^{-1}$	Plane strain (σ_2 lies in the fault plane) $\sigma_v = \sigma_1$ assuming an Andersonian extensional stress regime μ = 0.75 C ~ 2T	$(\sigma_1 - \sigma_3) \geq 5.66T$ (after Sibson, 1998)
Extension failure	$\lambda_v = (\sigma_3 + T)/\sigma_v$		$(\sigma_1 - \sigma_3) < 4T$, where T = tensile strength $P_f = \sigma_3 + T$
Hybrid extensional-shear failure	Griffith criterion $(\sigma_1 - \sigma_3)^2 = 8T(\sigma'_1 + \sigma'_3)$, where $\sigma'_1 = (\sigma_1 - P_f)$ and $\sigma'_3 = (\sigma_3 - P_f)$ $\lambda_v = [8T(\sigma_1 + \sigma_3) - (\sigma_1 - \sigma_3)^2]/16T\sigma_v$		$4T < (\sigma_1 - \sigma_3) \leq 5.66T$ (after Sibson, 1998)

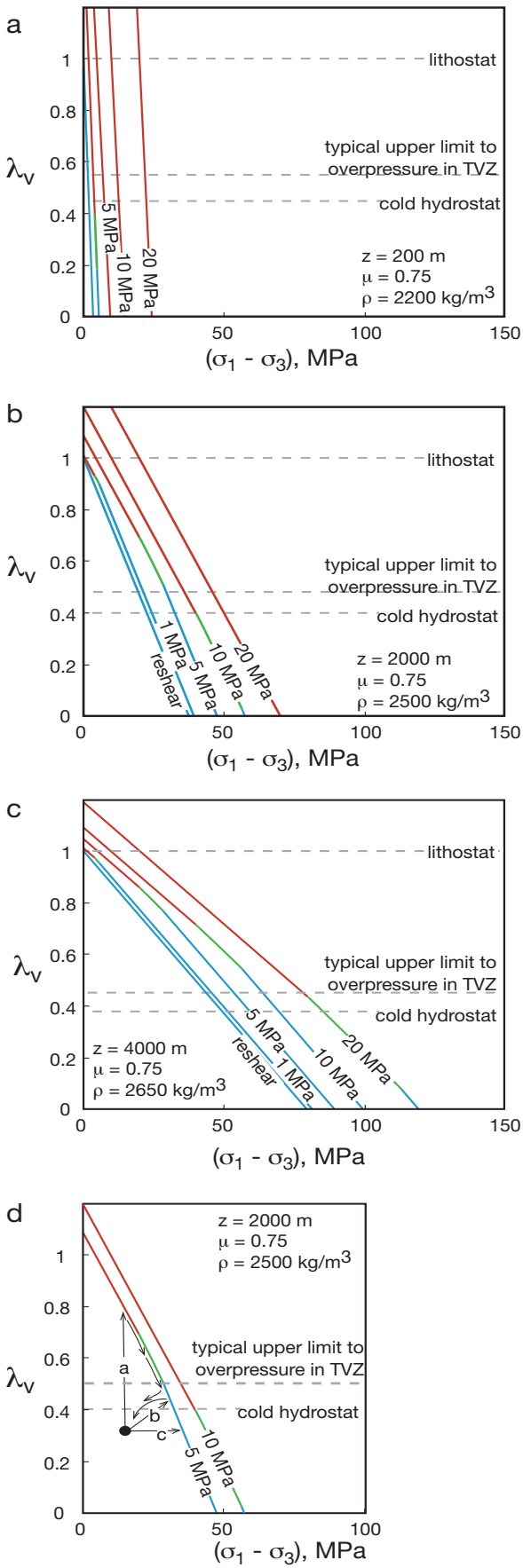

these inferred intersections there is complete loss of drilling fluid and the bit and drill string may drop by as much as 2 m, indicating open space. Crushed and brecciated rocks, many strongly silicified, invariably occur above and below these intervals and may be encrusted with quartz and adularia, typical of epithermal vein deposits. Fine-grained rocks, where present in drill core, have slickensides indicating normal or normal and/or strike-slip fault movement. These observations demonstrate that open structures, perhaps linked or dissected by faults, occur within the reservoir in zones of strong silicification. However, the vertical continuity of these high-flux conduits is unknown.

Figure 10d illustrates possible pathways to failure in λ-σ space for weak rock (T = 5 MPa) at a depth of 2,000 m. Failure conditions are shown for T = 5 and 10 MPa (the latter for comparison only). Depicted are three paths to failure from a common starting condition of hot hydrostatic pore fluid pressure and low differential stress (Cox, 2010). In scenarios where the pore fluid pressure builds up beneath seals, for example, in response to buoyant flow into closed or sealed fractures, pore fluid factor can increase rapidly relative to the rate of fault loading. Subsequent failure can then be largely pore fluid pressure-driven (e.g., path A, Fig. 10d). Continued tectonic loading drives the fluid pressure and stress state along the failure envelope, through the different failure regimes, as shown to occur in path A in Figure 10d. More generally, failure may be induced by a combination of changes in pore fluid factor and differential stress (e.g., path B, Fig. 10d). If the pore fluid factor does not change during the tectonic loading cycle, failure is purely stress driven (e.g., path C, Fig. 10d). The fact that Taupo Volcanic Zone geothermal systems generally do not exceed about 20% above cold hydrostatic pore fluid pressure imposes some constraints on possible pathways to failure. Inspection of Figure 10d shows that weak rock (T = 5 MPa) will fail only in shear at pore fluid factors less than this limiting condition. Moreover, purely pore fluid-driven failure is not possible from the starting conditions depicted. However, we know from seismic monitoring of fluid reinjection (e.g., Rotokawa: Heise et al., 2008), that pore fluid pressure-driven failure occurs at these depths. This implies that the starting conditions are critical and only small increases in pore fluid factor, or tectonic stress, are required to induce failure. Stronger rocks (e.g., T = 10 MPa) can fail in extension or extensional-shear at the same depth. In such cases, opening of extension fractures inhibits further build-up of fluid pressure. If shear failure occurs, both a stress drop and fluid pressure relief occurs. Feedback between pore fluid pressure

FIG. 10. (a)-(c). Plots in λ-σ space (after Cox, 2010), showing the effect of tensile strength on conditions for brittle failure in intact rock and conditions for reshear on a cohesionless preexisting fault optimally oriented for reactivation at 4000, 2,000, and 200 m depths within the Taupo Volcanic Zone. Plots are annotated with the lithostatic and cold hydrostatic pore fluid factors, and the maximum pore fluid factor generally observed within Taupo Volcanic Zone geothermal systems. (d). Possible pathways to failure in λ-σ space for weak rock (T = 5 MPa) at a depth of 2,000 m. Failure conditions shown for somewhat stronger rock (T = 10 MPa) for comparison. See text for discussion. Composite failure curves in all plots are color-coded according to macroscopic mode of brittle failure: red = extension failure, green = hybrid extensional-shear failure, blue = shear failure (fault).

and tectonic loading thus maintains fault-fracture pathways within the geothermal system.

Permeability within fault zones

Normal faulting, with perhaps a minor strike-slip component (Rowland and Sibson, 2001; Acocella et al., 2003), is the favored brittle failure mode within the Taupo Volcanic Zone and exerts the principal structural influence on fluid redistribution. Faulting and subsidence of the graywacke basement has had a large role in controlling the structural development in the cover sequence. Despite the lack of data on fault geometry at depth within the central Taupo Volcanic Zone, it is reasonable to infer that fault arrays at the surface comprise synthetic and antithetic splays that merge with major basement faults (e.g., Lamarche et al., 2006), and displacement likely increases with depth, as expected for growth faults. Much of the cover sequence is dominated by low-cohesion porous units; faults in this material are mechanically favored to develop clay-rich core (e.g., Caine et al., 1996), as are faults in any type of host rock with increasing displacement (Knott, 1993; Knott et al., 1996). Unfortunately, because complete profiles of fault zones are rarely observed, little work has been undertaken to quantify their permeability attributes. Observations are limited to low-displacement structures in high-porosity pyroclastic material or lake sediments, which have been accessed outside geothermal fields for paleoseismic purposes (e.g., Berryman et al., 2008). These faults generally are simple structures, perhaps with a thin (<10–20 cm) core of clay-rich gouge and few subsidiary fractures representative of a damage zone. Exhumation of fault zones in competent low-porosity rocks has yet to occur, and there are no descriptions from geothermal drilling. However, as reviewed by Micklethwaite et al. (2010), an increasing body of research indicates that permeability within fault zones may vary by over ten orders of magnitude, from bulk-rock values of ~10^{-20} to >10^{-16} m^2 (Manning and Ingebritsen, 1999; Townend and Zoback, 2000), up to co- and postseismic values estimated at 10^{-13} to 10^{-11} m^2 (Koerner et al., 2004; Miller et al., 2004). Gouge development, redistribution of material and sealing of gouge by pressure solution, and local redeposition of the dissolved material act to reduce permeability within the core of fault zones (Caine et al., 1996; Micklethwaite et al., 2010). Results of fracture-sealing experiments and observations of phenomena related to co- and postseismic fluid redistribution provide independent evidence to support the notion that seismically enhanced permeability is reduced over geologically short periods (days to years; Micklethwaite et al., 2010). In some cases, the reduction in permeability may be sufficient to impede flow across the fault surface during interseismic periods, as inferred to be the case at shallow depth (<50 m) at Orakeikorako (Rowland and Sibson, 2004).

In 1987, the M_L 6.4 Edgecumbe earthquake provided an opportunity to assess the co- and postseismic effects of a large normal fault rupture on the shallow hydrology of the Taupo Volcanic Zone, and particularly the Kawerau geothermal system, which lies immediately southwest of the fault rupture (Fig. 2). The pattern and timing of aftershock activity were consistent with the along-strike diffusion of a pore fluid pressure wave via fault valve behavior (Sibson, 1992). Such diffusion would have required transient permeability on the order of 10^{-11} m^2 afor low-porosity rocks (φ = 0.01) at depths near the base of the seismogenic zone (following Townend and Zoback, 2000). The uncertainty associated with this estimate is about an order of magnitude, allowing for variations in porosity. Even so, the transient rupture permeability is exceptional compared to the bulk permeability (~5×10^{-15} m^2) inferred for geothermal systems of the Taupo Volcanic Zone (McNabb, 1975; Fig. 9). Unfortunately, it is unknown if this earthquake induced fluid redistribution within the geothermal system. To date, this is the only large earthquake to have occurred within the Taupo Volcanic Zone since geothermal fluid production for energy began in 1958.

Fault zone complexity, rift architecture, and directional permeability

The permeability distribution within fault zones is affected by fault growth and interaction (Curewitz and Karson, 1997), and structural overprinting (e.g., Berger et al., 2003). As a result, fluid flow may be directed through interconnected fault-fracture networks within spatially more extensive fault and/or fracture systems. Fault irregularities in the direction of slip, for example, may lead to the development of highly permeable dilational zones within extensional stepovers, or jogs (Sibson, 2001). In extensional settings, jogs focus fluid flow along strike (parallel to σ_2), and in strike-slip settings, jogs form subvertical pipes (Sibson, 2000). The efficacy of the latter situation for localizing hydrothermal flow has strongly influenced structural interpretations of epithermal orebodies (e.g., Henley and Adams, 1992; Berger et al., 2003). However, pipelike zones of enhanced permeability also develop as a consequence of normal fault growth and linkage, perhaps explaining the development of subvertical zones of vein dilation in some extensional epithermal settings (e.g., Nortje et al., 2006). Fault growth and linkage generates and tectonically maintains subvertical zones of enhanced permeability at relay zones between normal fault segments, transfer fault intersections with rift faults, and lateral fault tips (Curewitz and Karson, 1997), and as a consequence of vein corrugations and changes in kinematics that may occur from slip event to slip event (Micklethwaite, 2009).

Additionally, directional permeability may be imposed at the regional scale by rift architecture. Regions under extension tend to break into segments comprising subparallel arrays of normal faults and, if magma is present, deeper seated dike swarms (e.g., Dabbahu rift, Afar: Rowland et al., 2007; Main Ethiopian rift: Ebinger and Casey, 2001). In general, segmentation scales with the thickness of the mechanical layer that is breaking (Ebinger et al., 1999). Displacement between segments must be accommodated, either via transfer faults oriented at high angle to the axis of rifting, in which case the segments are said to be "hard-linked" (Gibbs, 1984), or by distributed deformation and small-scale faulting within the blocks between adjacent segments, which is termed "soft-linkage" (Rosendahl et al., 1986; Morley at al., 1990). In either case, these accommodation zones tend to be basement highs in the context of the entire rift system. The bulk permeability in rift segments contrasts with that in accommodation zones (Rowland and Sibson, 2004). This is a function of the cumulative effect of subparallel faults and fractures in the former and structurally favorable sites for enhanced vertical

permeability in the latter. An array of faults and fractures has much the same effect on bulk permeability as stratigraphic layering: permeability across the strike of the array is lower relative to other directions, regardless whether faults behave as conduits or baffles to flow. When superimposed upon a layered sequence, the combined effect is to reduce vertical and across-strike permeability relative to along-strike permeability (Fig. 11). In contrast, all favorable structural sites for

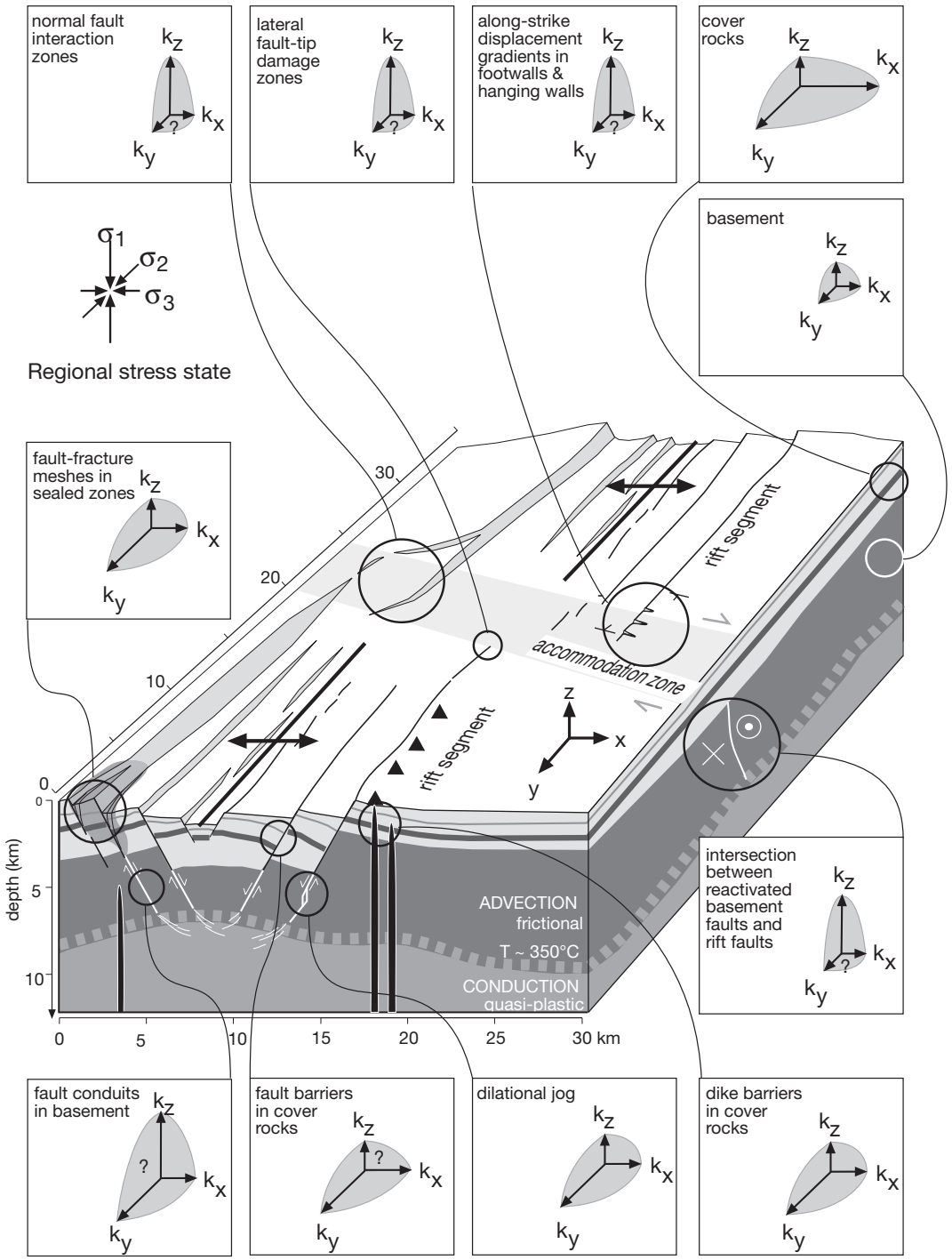

FIG. 11. Schematic block diagram illustrating the effect of structures on permeability anisotropy in the central Taupo Volcanic Zone, assuming a simple layered cover sequence overlying a competent basement with low intrinsic permeability (Rowland and Sibson, 2004). Schematic three-dimensional permeability diagrams depict relative magnitudes of mutually perpendicular across strike (x), along strike (y), and vertical (z) permeability for different structural settings within the rift system. Relative magnitudes are indicative only. Question mark between arrows indicates uncertainty in the relative magnitude of adjacent directional permeabilities. Settings with enhanced and localized vertical permeability are favored in accommodation zones.

focused vertical flow occur within accommodation zones (e.g., rift fault-transfer fault intersections, lateral fault tips on first order structures, and linkage zones between first-order structures: Fig. 11). Rift architecture thus may modulate fluid-flow paths such that upflow zones are favored in accommodation zones and recharge and axial flow is favored in rift segments (Rowland and Sibson, 2004).

The fault pattern in the Taupo Volcanic Zone is consistent with this style of rift architecture. Rift segments are on the order of 20 km long, as expected for a brittle crust approximately 6 to 10 km thick (Fig. 1b; Ebinger et al., 1999; Rowland and Sibson, 2004). These segments are not hard-linked at the surface but the accommodation zones coincide with the position of inferred basement structures (Fig. 12a; Wan and Hedenquist, 1981; Cochrane and Wan, 1983; Rowland and Sibson, 2004), which are favorably oriented for reactivation as transfer faults (Ring, 1994; Morley, 1999; Le Turdu et al., 1999). It is possible that the Taupo Volcanic Zone is soft-linked within the young cover sequence but hard-linked at depth.

The distribution of geothermal fields within the Taupo Volcanic Zone suggests structurally influenced directional permeability, at least to some extent. Taking the 30 Ωm (500 m electrode spacing) resistivity contour as a reasonable proxy for the outer boundary of the geothermal system at 500 m depth (Bibby et al., 1995), inspection of Figure 12a demonstrates that many (60% according to Rowland and Sibson, 2004), geothermal fields are co-located in accommodation zones, but none occur within the fault belt. Of the geothermal systems discussed in this paper, Te Kopia occurs on subsidiary structures at the lateral tip of the Paeroa Fault, and Orakeikorako straddles the linkage zone between this structure and another large normal fault to the southwest (Fig. 7). These two geothermal systems are optimally positioned for the localized and tectonically maintained development of subvertical high-flux conduits. The extinct Ohakuri geothermal system occurs within an accommodation zone, and it is positioned where the modern rift intersects a major basement feature—the southern projection of the eastern margin to the Hauraki rift (Fig. 12a). Waiotapu and Waimangu lie at the intersection between the Paeroa Fault (and its associated splays), the Kaingaroa Border Fault, which offsets basement graywacke by over 2,000 m, and an inferred basement cross structure (Cochrane and Wan, 1983).

However, structural influence is not obvious within the Taupo-Reporoa Basin (TRB, Fig. 1), which is notable for its lack of rift architecture, extraordinarily high natural heat output, and thick accumulations of weak and porous pyroclastic deposits and their reworked equivalents. There is a higher density of geothermal fields within and more generally on the periphery of this basin than anywhere else in the Taupo Volcanic Zone, perhaps because it is the current locus of arc volcanism (Rowland et al., 2010). The lack of obvious structural control at the surface may reflect the masking effect of the basin fill, which in this region comprises much of the stratigraphic pile within the convective regime. Regardless, the tendency of geothermal fields to occur around the margin of the basin (e.g., Broadlands-Ohaaki, Rotokawa, Waiotapu, Te Kopia, Orakeikorako,) or where accommodation zones may produce basement highs (Wairakei-Tauhara, Ngatamariki) suggests deep-seated control by inherited basement faults. These structures are of particular importance because they likely root in creeping and thus potentially permeable, shear zones within the ductile lower crust and may therefore channel fluids across the brittle-ductile transition zone (Cox et al., 2001).

Magmatism and volcanism

Magmatic and volcanic processes influence fluid redistribution within the central Taupo Volcanic Zone, first, by providing heat to drive hydrothermal convection, and second, by modifying permeability networks. The predominance of rhyolitic volcanic products attests to the importance of a mid-crustal "hot zone" (Fig. 12e), which is intruded by mantle-derived basalt and/or its hybridized daughter products (e.g., Annen et al., 2006). Occasionally, basalt dikes transect the entire crustal section (e.g., Tarawera basalt eruption, 1886; Nairn and Cole, 1981), but most mafic magma is trapped within or below the hot zone, contributing to the generation and eruption of silicic melts (Nairn et al., 2004; Shane et al., 2007), and feeding the high heat flow of the region (4,200 MW_{th}; Bibby et al., 1995; Hochstein, 1995). Geochemical variations in post-61 ka eruption products from the Taupo and Okataina volcanoes (Charlier et al., 2005; Smith et al., 2005) demonstrate that the hot zone is highly heterogeneous and likely comprises a plexus of dikes, sills, pods, and mushy differentiated intrusions (Rowland et al., 2010), similar to the MASH (melting, assimilation, storage, and homogenization)

FIG. 12. Regional-scale controls on the localization of geothermal activity within the central Taupo Volcanic Zone. (a)-(d). Maps show the distribution of geothermal systems, as delimited by the 30 Ωm resistivity contour (red line) in relationship to (a) active fault pattern (fine black lines), modern rift axes (blue dashed lines), inferred basement faults (gray lines), active calderas (TA = Taupo, OK = Okataina), and lakes (light gray lines); (b) distribution of <61 ka volcanic vents, shown by circles (white = rhyolitic, orange = andesitic) and squares (red = basalt, dike if linked by red line), and speculative areal extent of a midcrustal hot zone, as shown in (e); (c) active (solid black line) and inferred (dashed black line) caldera boundary faults; (d) metal flux for selected systems (after Simmons and Brown, 2007); (e) composite profile constructed for a representative section, position shown by ball-end line in (a), and speculative fluid-flow model across the central Taupo Volcanic Zone incorporating geophysical data (Sherburn et al., 2003; Rowland et al., 2010), structural data, and major features of the lithospheric-scale conductivity model of Heise et al. (2007). Boundary between frictional upper crust and quasiplastic zone is defined as the level above which 80% of earthquakes occur and is not well resolved. Yellow areas indicate upflow zones. Blue arrows show recharge zones. Red dashed line and red crosses indicate intrusions inferred from fast seismic wave speed. Inferred hot zone shown by pink region within mid crust, and it overlies a high conductive zone containing melt (Heise et al., 2007). The vertically exaggerated topographical profile is annotated with major faults, structural features, and heat output, which is summed in 5 km wide strips across the Taupo Volcanic Zone and collapsed onto the profile line (from Bibby et al., 1995).

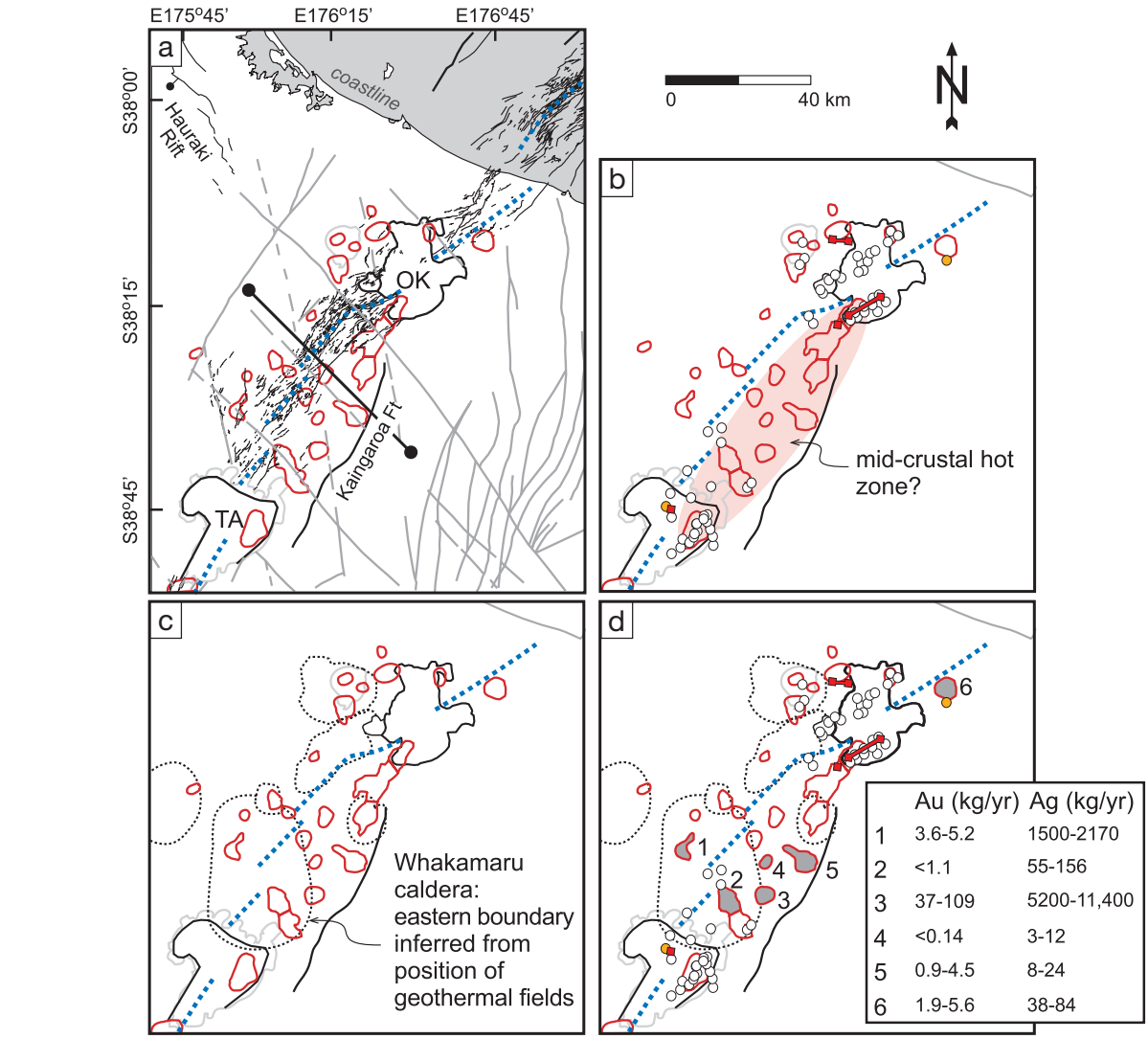
E175°45'
E176°15'
E176°45'
S38°00'
S38°15'
S38°45'
a
coastline
Hauraki Rift
OK
Kaingaroa Ft
TA
0
40 km
N
b
mid-crustal hot zone?
c
Whakamaru caldera: eastern boundary inferred from position of geothermal fields
d
1
2
3
4
5
6
Au (kg/yr) Ag (kg/yr)
1 3.6-5.2 1500-2170
2 <1.1 55-156
3 37-109 5200-11,400
4 <0.14 3-12
5 0.9-4.5 8-24
6 1.9-5.6 38-84

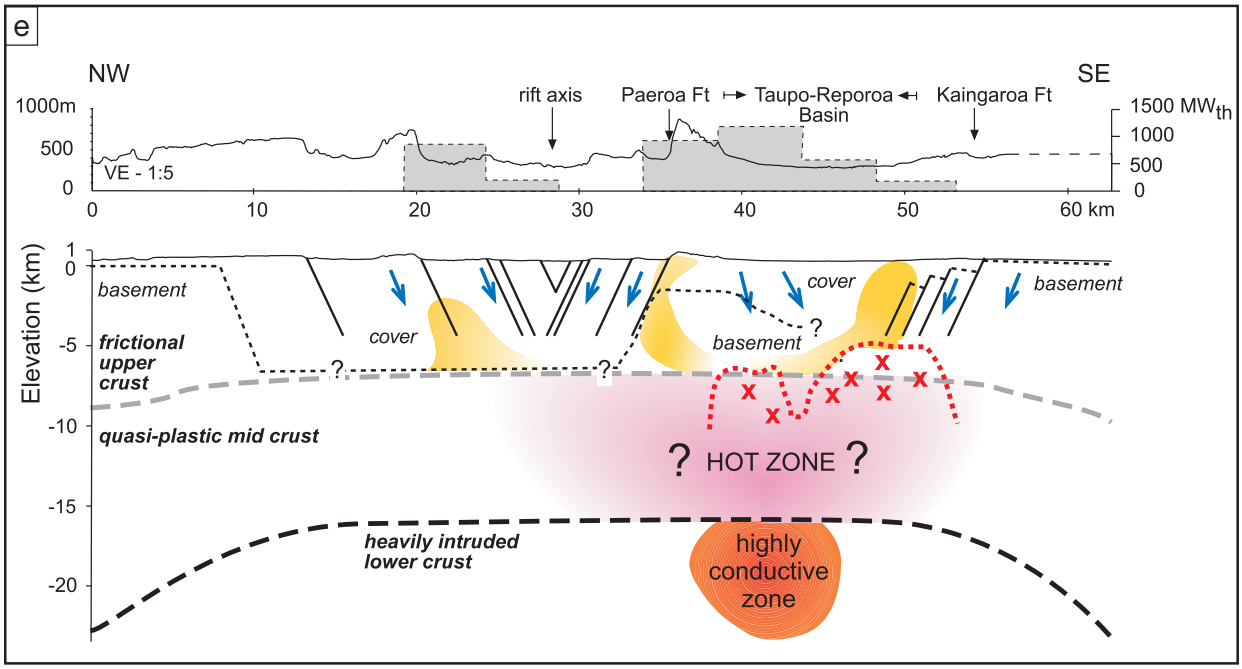
e
NW
SE
1000m
500
0
VE - 1:5
rift axis
Paeroa Ft
Taupo-Reporoa Basin
Kaingaroa Ft
1500 MWth
1000
500
0
0
10
20
30
40
50
60 km
Elevation (km)
1
0
-5
-10
-15
-20
basement
frictional upper crust
quasi-plastic mid crust
heavily intruded lower crust
cover
basement
cover
basement
? HOT ZONE ?
highly conductive zone

zone of Hildreth and Moorbath (1988). Feedback between melt extraction and crystallization imparts a degree of geometrical and thermal stability to the hot zone, so that over much of its dimension and for much of its duration, it is buffered between the solidus and liquidus for its local compositions (Hildreth, 1981; Annen et al., 2006).

The dimensions of the hot zone are unknown. However, given the exceptional heat flux (>2,000 MW) through the Taupo-Reporoa Basin, plus the evidence for partial melt in the deep crust beneath (Heise et al., 2007), it together with Taupo Volcano and the Okataina volcanic center likely encompass the areal extent of the modern hot zone (Fig. 12b). The depth dimension of the hot zone can be inferred from seismic and electrical properties of the crust, and it likely extends across the full depth of the midcrust down to ~16 km depth (Fig. 12e; Bibby et al., 1995; Harrison and White, 2004, 2006; Stratford and Stern, 2004, 2006). The potential volume of the hot zone is supported by the occurrence of clustered large caldera eruptions. From 340 to 230 ka, after a ca. 370 kyr period during which no major ignimbrites are known to have been erupted, at least seven ignimbrite-forming and numerous smaller eruptions occurred, totaling >3,000 km^3 of magma and forming calderas that pepper a 90 × 40 km area (Rowland et al., 2010).

During the past 61 ka about 780 km^3 of predominantly silicic magma has erupted in the central Taupo Volcanic Zone, of which ~80% was released in three moderate to large caldera-forming eruptions at 61, 26.5, and 1.8 ka (Wilson et al., 2010b). Studies on Taupo and Okataina Volcanoes demonstrate that the melt-dominant rhyolite magma bodies disgorged during such eruptions are lodged at shallow levels (~4 to <10 km deep: Dunbar et al., 1989; Liu et al., 2006; Shane et al., 2008). In addition to the active Taupo and Okataina Volcanoes, six older calderas have been inferred within the central Taupo Volcanic Zone (Fig. 12c). Faults related to caldera collapse therefore are common and provide cross-stratal pathways to the depth of the melt storage zone. One-third of all geothermal fields lie on well-defined caldera boundary faults, but it is difficult to ascribe a genetic link because some of these structures have been delimited from the distribution of geothermal fields (e.g., eastern margin of Whakamaru caldera; Fig. 12b). Waiotapu and Waimangu are the least equivocal examples of fluid flow localized along caldera ring faults. At Waiotapu, a cluster of hydrothermal eruption craters, including Champagne Pool, occurs where the ring fault at the northern margin of the Reporoa caldera is inferred to cross the geothermal field (Fig. 4). Lake Whangioterangi fills two of these craters and forms an E-W–striking feature, which is online with the inferred caldera structure. At Waimangu, the site of the Pink and White Terraces, and the locus of surface discharge surrounding ancestral Lake Rotomahana before the 1886 eruption, lie on the Haroharo caldera structure (Fig. 6).

Magma transport via dike intrusion also may affect fluid flow. Dikes may propagate up into the convective regime and either stall and crystallize or erupt (e.g., 1886 Tarawera eruption; Rowland et al., 2010). Fracturing ahead of a propagating dike enhances permeability (Rowland et al., 2007), perhaps triggering hydrothermal eruptions (e.g., Nairn et al., 2005), and may provide high-flux structurally controlled fluid conduits in the aftermath of the intrusion, as may cooling joints formed along intrusive margins (Lister, 1974). Dikes that drive fissure eruptions also may enhance vertical permeability through the development of pipelike volcanic vents as is evident at Waimangu.

Despite the apparent association between geothermal systems and calderas or dikes, the occurrence of major eruptions and intrusions does not necessarily affect the deep permeability structure. For example, the Wairakei geothermal system appears to have been unchanged in its position despite nearby plinian eruptions from Taupo Volcano (Bibby et al., 1995), and Waimangu was well established prior to the 1886 Tarawera eruption, as demonstrated by the existence of the Pink and White Terraces. Thus, deep geothermal circulation in the central Taupo Volcanic Zone appears to be relatively stable despite being punctuated by a range of volcanic and magmatic events.

Conceptual Model for Hydrothermal Flow from Feed Zone to Surface

Hydrologic, magmatic, and tectonic processes above and below the epithermal environment control the formation of high-flux conduits where precious metals accumulate. For the discussion that follows, we examine these processes over three overlapping but distinct depth intervals from the surface to the base of the convection cell (Fig. 13). These are designated the feed zone, the epithermal zone, and the discharge zone. The epithermal zone is the interval in which precious metal mineralization develops in high-flux subvertical fluid conduits. Such conduits are pipelike and over time can coalesce into a vein. The feed zone is where the roots of the high-flux conduits form, and the discharge zone is where they branch and disperse. Two features are important. First, the fault-fracture network develops across the entire vertical extent of the hydrothermal plume, transecting all three zones. Second, from time to time pipelike high-flux conduits develop within this network, tapping deep fluid in the feed zone and transmitting it through the epithermal zone upward to, and possibly through, the near-surface discharge zone.

Feed zone (>2,000 m depth)

The feed zone extends from >2,000 m depth to the brittle-ductile transition and the base of fluid convection. The details of the geologic context are sketchy, but we can constrain a number of aspects based on near-surface observations. Low-porosity rocks comprising basement and the lower part of the Quaternary volcanic sequence limit fluid movement to fault-fracture networks. The pressure gradient is probably slightly greater than hydrostatic, with possible transient excursions. The temperature gradient is near isothermal, assuming the rising fluid and surrounding country rock are in thermal equilibrium as expected for a mature geothermal system. At these pressure-temperature conditions boiling is suppressed, and the hydrothermal fluid is a liquid phase. In addition, this fluid has a composition that permits transport of significant concentrations of precious metals. The main factors constraining fluid flow are (1) magmatic intrusion, which mainly supplies heat and energy, but which can also facilitate fracture extension at the tip of a dike; (2) proximity to the brittle-ductile transition, which limits the downward flow of water; (3) the

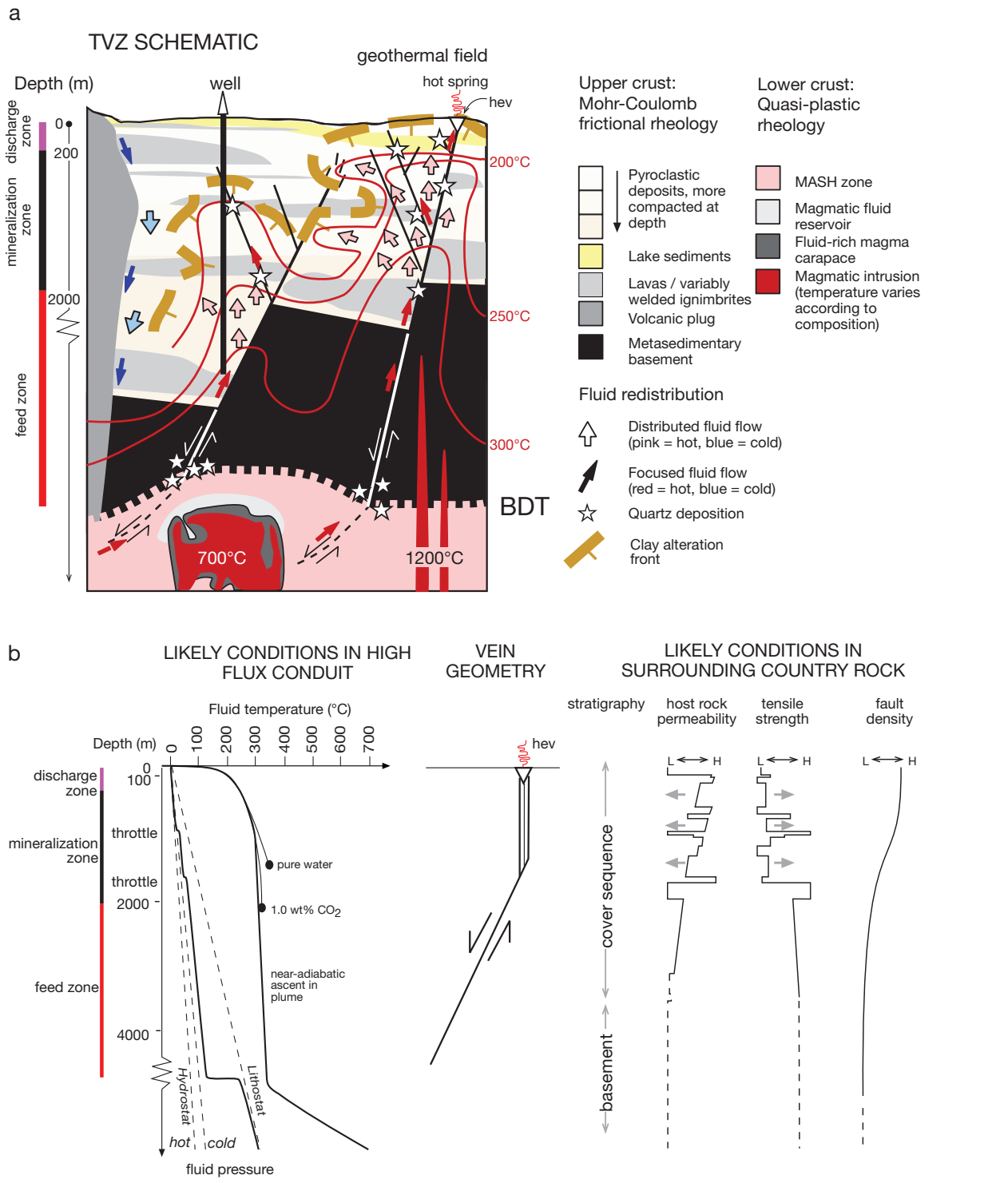

FIG. 13. (a). Schematic section showing likely fluid-flow conditions within a geothermal system, which transects a relatively impermeable basement and an overlying cover sequence, which comprises weak and porous lithologies intercalated with and punctured in places by more competent and less permeable layers. BDT = brittle-ductile transition; hev = hydrothermal eruption vent. Color-coded depth intervals represent the discharge zone, epithermal mineralization zone, and feed zone discussed in the text. (b). Expected temperature and pressure conditions in a high-flux vertical conduit, such as a well as located in (a) or an epithermal vein with geometry as shown, and variations in natural conditions with depth for a location nearby. The position and gradient of the transition between hydrostatic and lithostatic pressure is uncertain but is probably located between 5 and 8 km depth. L = low, H = high, gray arrows indicate the effects of mineral deposition (ground preparation) on the natural conditions.

tensile strength of host rocks which is generally high; and (4) hydrostatic fluid pressure, which is maintained because brittle failure relieves the build-up of fluid overpressures.

We infer that the dimensions of magmatic intrusions are highly variable, ranging from broad cylindrical plugs to narrow dikes and sills (e.g., Smith et al., 2004; Charlier et al., 2005; Ellis et al., 2007; Smith et al., 2007), and that the sites of intrusion can localize the positions of the hydrothermal plume (Bibby et al., 1995; Christenson et al., 2002). Although most melts presumably stall and/or crystallize at midcrustal depths, some clearly intrude the hydrothermally active upper crust (e.g., Nairn and Cole, 1981; Browne et al., 1992; Nairn et al., 2005). Tectonic control influences magma emplacement and heat and mass transfer, as demonstrated by the strong NE- and NW-trending alignments of post-61 ka vents (Fig. 12b; Wilson et al., 2010b), and it is conceivable that such coupling of structure and igneous intrusion is a major control on the localization of the sites of geothermal convection cells (Fig. 13).

Provided the contrast in permeability is sufficient, buoyant fluid flow and recharge within the cover sequence may be guided by the juxtaposition of basement blocks against more permeable volcaniclastic materials. Alternatively and arguably more likely at this depth for reasons discussed earlier (Fig. 10c), hydraulic connectivity will be fault controlled via structures favorably oriented for reactivation in the prevailing stress field (Townend and Zoback, 2000). For NW-SE–directed extension, NNE- to ENE-striking structures of moderate to steep dip (45°–90°) and WNW- to NNW-striking subvertical structures are favored to reactivate as normal and strike-slip faults, respectively. Basement fault zones probably have a complex internal permeability structure (baffle or conduit) that is strongly affected by the structural and metamorphic fabric of the host rock and total displacement (and therefore development of fault gouge). Fluid flow may be inhibited, locally inducing overpressures (Byerlee, 1993), which may be relieved by episodic fault-valve activity related to the seismic cycle (Sibson, 1992), as suggested by the prevalence of seismic swarm behavior (Sherburn, 1992).

Within this environment, the temperature gradient is probably adiabatic except close to the brittle-ductile transition, where heat transfer changes from convection above the transition to conduction below it (Fig. 13b), and where partially to fully sealed conduits induce elevated pore fluid pressures. Except for these sites, mineral deposition is minimal and preexisting faults with significant gouge development can be expected to remain weak over much of their vertical extent and, therefore, prone to reactivation. These structures presumably root in creeping shear zones in the ductile midcrust. This is particularly likely because the depth to the base of the seismogenic zone has lessened through time as a result of thermal weakening (Villamor and Berryman, 2006). Creep on these shear zones may dynamically enhance permeability within the ductile regime, providing a suitable mechanism for channeling any overpressured liquids across the brittle-ductile transition via the fault-valve mechanism (Fig. 13; Sibson, 1992; Cox et al., 2001).

Epithermal mineralization zone (<200–2,000 m depth)

The epithermal zone is the depth interval in which boiling conditions develop and high-flux conduits form, and additional fluid buoyancy can derive from two-phase fluid flow in narrow, vertical fractures or pipes. Accepting these conduits are analogous to a geothermal well, they are likely open over a long vertical interval (>1 km), and they must be isolated from shallow-water inflows in the same way that well casing works. As discussed in the next section, such high-flux conditions are likely short-lived and transient. For much of the duration of hydrothermal fluid flow, however, the main controlling factors are (1) presence and/or development of a vertically extensive fault-fracture network; (2) the primary porosity-permeability of host lithologies; (3) heterogeneities in the tensile strength of the host rocks and their ongoing transformations (both weakening and strengthening) due to hydrothermal alteration, which affect the mode of brittle failure; (4) the basement faults which localize growth faults in the cover layer; and (5) complexity arising from interplay of lithologic and structural controls on fluid movement.

Within the epithermal mineralization zone of the central Taupo Volcanic Zone, the stratigraphy is dominated by weak volcanic rocks which favor the development of clay-rich cores in faults with large displacements, except locally where faults cut competent lavas and welded ignimbrites. In general, faults in this zone will behave as baffles causing compartmentalized fluid flow, which is distributed within fault blocks (e.g., Orakeikorako: Rowland and Sibson, 2004), and accounts for large volumes of hydrothermal alteration (10–≥100 km^3). The development of vertically contiguous and increased permeability is possible following large seismic events that rupture the entire thickness of the convective zone (e.g., 1987 M_L 6.4 Edgecumbe earthquake: Smith and Oppenheimer, 1989). However, with the exception of a few locations dominated by domes, and in the absence of large-volume silicification, it is doubtful that the permeability contrast between the host rock and the fault zone would be sufficient to maintain focused and high flux flow across the full vertical interval of the cover sequence for time periods much in excess of the postseismic phase (the period—days to months—during which the rock volume experiences aftershocks in response to viscoelastic relaxation after a major earthquake: Omori, 1894). Dike injections into and across this depth interval additionally may drive development of high-permeability pathways, either in open fractures above and ahead of the dike as discussed above, or via cooling joints along dike margins.

Discharge zone (surface to <200 m depth)

The shallow depth interval from the surface to less than 200 m depth incorporates the environment where mineralized vein structures branch and terminate upward (e.g., Simpson and Mauk, 2007). Fluid pathways to the surface tend to be localized on hot-spring conduits and hydrothermal eruption vents, crosscutting zones of clay alteration (Fig. 13). The hydrology is complex (e.g., Fig 3) and the main factors that constrain fluid flow are (1) presence of low tensile-strength rocks (i.e., weak, cohesionless pyroclastic rocks or rocks undergoing clay alteration), which are poorly suited for development of open fractures; (2) low differential stress which promotes development of short (<100 m) permeable fractures of almost any orientation (e.g., Cosgrove, 1995); (3) silica deposition which can isolate vertical pipes that supply fluid to hot springs; and (4) interplay between cold water aquifers and

ascending columns of hot water, which generates a fingering effect that breaks up the flow and discharge of hot water into discrete hot springs. Ingress of cold water can occur in zones of high permeability (Figs. 3, 4).

As is evident from the geothermal fields described earlier (Figs. 3–7), the locus of the strongest surface thermal activity is not necessarily located centrally. Rather, it can be located on the edge of the resistivity boundary and localized on high fluid-flow structures that transect the underlying epithermal zone. Given that mineral deposition can fill these structures rapidly, hydrothermal fluid flow appears to be sustained by episodic and explosive eruption of boiling hot water, which reopens fluid pathways to the surface.

Epithermal Vein Formation: Spatial and Temporal Considerations

Ore-hosting epithermal veins containing quartz ± adularia ± calcite are small compared to the overall size of the hydrothermal plume, as delimited by the volume of hydrothermal alteration in which they form (Simmons et al., 2005). In their simplest geometry, they comprise steeply dipping structures, resulting from extension and extensional shear (Fig. 13b). Precious metal orebodies are generally 500 to 2,000 m in strike length, 1 to 3 m wide, and 300 to 500 m in vertical dimension. They form at <300°C and <2-km depth in zones with very high, vertical permeability that seems rare in the context of what has been observed in the Taupo Volcanic Zone, except in production wells which provide the best analogy in terms of fluid flow and favorable conditions for metal deposition. To illustrate the space-time dimensions of vein mineralization, we consider the fluid budget needed to fill a 1-m-wide vein, 1,000 m long, and 500 m high with quartz (1.3×10^6 t) and 1 million oz of gold (31 t). Approximately 290 mg of quartz deposits from 1 kg of solution that cools via adiabatic boiling from 260° to 180°C (e.g., Simmons and Browne, 2000), thus requiring 4.5×10^9 t of solution to form the model vein. At an upflow rate of 100 kg/s (3.1×10^6 t/y), it would take ~1,400 years to supply all the silica to fill the vein. Similarly, it would take ~1,000 years to supply all the gold, assuming the same deeply derived hydrothermal solution flowing at 100 kg/s contains 10 μg/kg gold, comparable to the amount measured at Rotokawa (Simmons and Brown, 2007), and >99% of the metal precipitates over the 260° to 180°C boiling interval as seen at Broadlands-Ohaaki (Brown, 1986).

For these calculations, the fluid flow localized in the model vein is consistent with the production from a single well with 9-5/8" production casing. It is also at the low end of values for natural deep flow supplying geothermal reservoirs at 0.6 to 2.5 km depth (Table 1). If a large volume of fluid is available at <3 km depth in the country rock (as in a geothermal reservoir), then the time period required to fill an epithermal vein might be substantially shorter. For example at Wairakei, after 50 years of fluid production (1958–2008) through 40 to 50 wells, about 3 km^3 of hydrothermal water (>250°C) was extracted from the reservoir covering an area ~10 km^2 (Bixley et al., 2009). If the aqueous gold concentration is 10 μg/kg and the solution is quartz saturated, this mass of water could supply about 23 t of gold (~750,000 oz) and 0.67×10^6 t of quartz. The calculations above indicate that the time required to fill a vein with substantial amounts of gold and quartz is short on the time scale of several tens to a few thousand years. This means that within the lifespan of a geothermal system of several hundred thousand years, structures conducive to vein formation could lie dormant due to mineral sealing with near stagnant flow for long periods of time, possibly up to several tens of thousands of years or longer (e.g., Sanematsu et al., 2006), separated by short spasms of high flow. Moreover, if the analogy with a producing geothermal well is appropriate, the dimensions of the openings required to generate focused flow through a channel can be narrow in width and short in along-strike extent, notably shorter than the dimensions of many epithermal veins, but long in vertical dimension (>1,500 m) and possibly pipelike. Accordingly, multiple episodes of structural dilation, high fluid flux, and mineral deposition most likely account for the resulting dimensions of vein orebodies, while turbulent pulsating two-phase flow contributes to the diversity of mineral textures (Simmons et al., 2005). The deep hydrothermal supply of precious metals is also likely to fluctuate but perhaps not in phase with development of high-flux conduits.

The active epithermal environment thus is characterized by two end-member hydrologic conditions: tortuous flow networks with long pathways (>>2,000 m), providing sufficient permeability to satisfy the condition for fluid convection (Fig. 14a); and a discrete steep to vertical structure that focuses decompressional boiling in the upflow zone of the system (Fig. 14b-c). The first condition involves buoyancy driven by large-scale differences in density between hot and cold water and can be considered "quasi steady-state" over the lifespan of the geothermal system. Buoyancy may fluctuate according to deep magmatic input, but the bulk permeability is probably buffered about the limiting condition for convection ($k > 10^{-16}$ m^2) by feedback between porosity modification through fluid-rock interaction, pore fluid pressure fluctuations, and tectonic stress cycling, particularly in the feed zone to the epithermal environment. The bulk permeability accounts for the large volume of zoned hydrothermal alteration that forms in the epithermal environment (e.g., Broadlands-Ohaaki). The second condition is transitory, and it is the natural analogue to the geothermal well in which fluid flow is associated with the vertical expansion of a two-phase column of boiling fluid. High-flux conduits conducive to epithermal vein formation only have to form episodically to account for the deposition and accumulation of large amounts of precious metal, but the timing of high flow conditions must be linked with the deep hydrothermal supply of gold and silver.

Two scenarios for the development of transient high-flux conduits are depicted in Figure 14—tectonic fault activation and an increment of dike intrusion. The strain associated with the latter scenario is particularly favorable for development of large-aperture fractures, as is evident from the following comparison. The M_L 6.4 1987 Edgecumbe earthquake in the northern Taupo Volcanic Zone was associated with a horizontal extension of approximately 1 m (Anderson et al., 1990). The Edgecumbe fault dips to the northwest at 45° ± 10°, and the rupture initiated at ~8-km depth (Anderson et al., 1990). Thus the hanging wall to the fault extends across a region ~8 km in width. Although the extension was mostly accommodated by shear along this fault and open-mode fractures where it intersected the surface, subsidiary structures within

the 8-km-wide hanging-wall block also were activated. In contrast, the dike intrusion associated with the 1886 Tarawera eruption may have accommodated twice this amount of extension (Rowland et al., 2010). The point here is that had the dike stalled at depth it would have localized faulting and fracturing in the brittle carapace above the level of intrusion to a region probably no wider than twice the depth to the level of intrusion (Pollard et al., 1983). Stalled dikes thus may generate very high brittle strains and are particularly suitable for the development of open fractures (Fig. 14c).

Regardless of extension mechanism (purely tectonic versus dike-induced faulting), the maximum opening in any single event is unlikely to exceed a meter or two. The generation of large veins (width >>1 m) thus must involve cycles of fault reactivation. Two observations are relevant to this point. First, reactivation of steeply dipping normal faults with large opening components, expressed at the surface by >1-m-wide fissures, occurs in association with repeated increments of dike intrusion in regions dominated by magmatic rifting (e.g., Dabbahu rift, Afar: Rowland et al., 2007). Second, in an established tectonic regime, and in the absence of magma throughput, extension is predominantly accommodated by reactivation of weak faults (cf. Sibson, 1985; Rowland et al., 2010). Provided that a vein is connected to a weak larger scale structure that is favorably oriented for reactivation, numerous episodes of opening and subsequent sealing are likely.

In the Taupo Volcanic Zone, Frying Pan Lake at Waimangu has hydrothermal flow conditions that most closely approximate those of a geothermal production well and an epithermal vein. Hydrothermal activity at Frying Pan Lake was a direct product of dike intrusion during the 1886 eruption of Mount Tarawera, which facilitated fracture dilation along a preexisting structure and which initiated outside the hydrothermal plume and migrated across its northern edge. The resulting pipelike conduits promote focused vertical fluid flow that is conducive to boiling and epithermal mineralization. At Rotokawa, the NE-SW alignment of large hydrothermal eruptions over a ~1-km distance indicates explosive episodic hydrothermal heat and mass transfer over a period of at least ~22,000 years along a narrow structure that extends to >400 m below the surface. Combined with substantial hydrothermal transport of precious metals (Simmons and Brown, 2007), this setting has the essential ingredients of epithermal

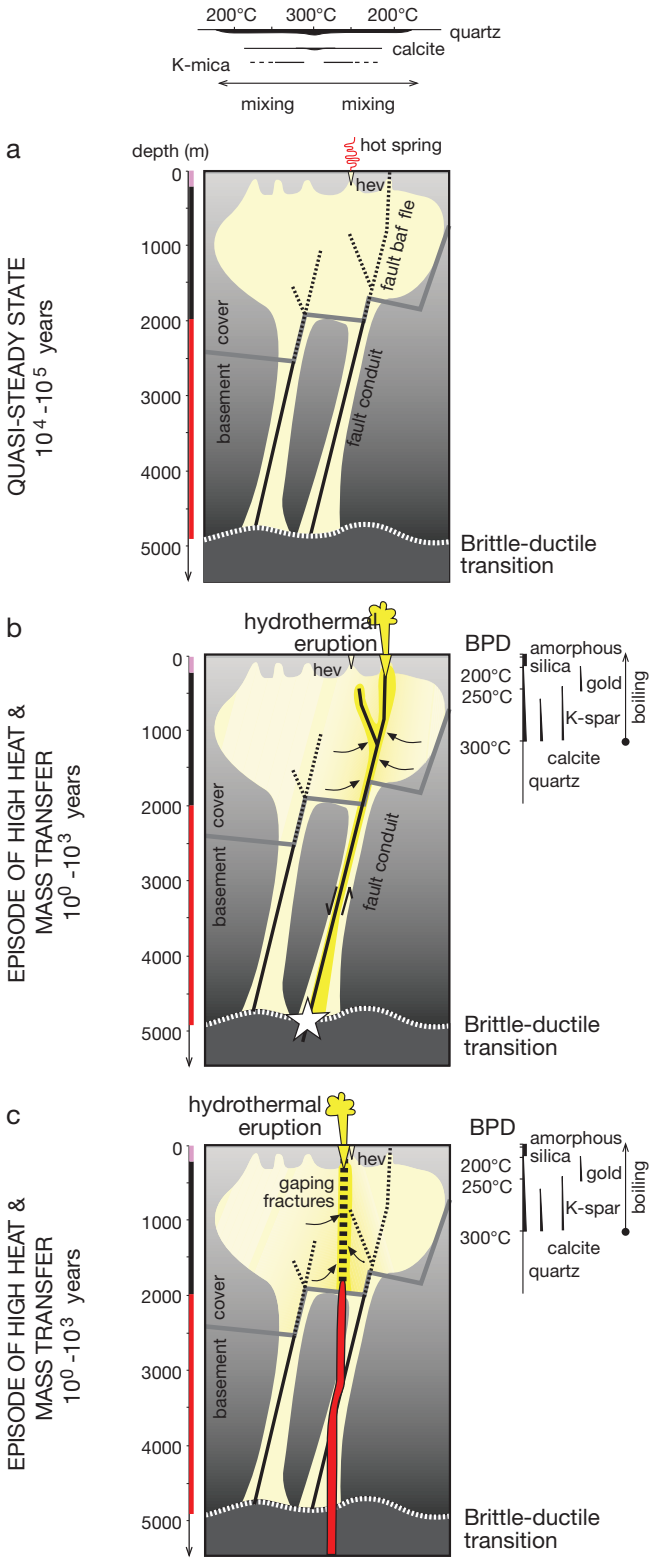

FIG. 14. Cartoon illustrating the tectonic and magmatic processes influencing high-flux fluid flow in a geothermal system and the epithermal environment (hev = hydrothermal eruption vent). (a). Quasi steady-state condition. Fluid flow is distributed through a large volume within the cover materials and inactive faults, or those that are in their interseismic phase (dashed), behave as baffles to flow, compartmentalizing the reservoir. Old hydrothermal eruption vents localize surface discharge. This condition produces a large volume alteration halo (yellow), plus possible low-grade disseminated epithermal mineralization. The distribution of minerals that result from mixing and cooling within the alteration halo is shown above the diagram, assuming for simplicity that upflow is centrally positioned within the plume (Simmons and Browne, 2000). In basement rocks, upflow is focused through faults and fractures well oriented for reactivation. (b). Transitory condition in which a high-flux fault conduit is generated (or reactivated) across the convection regime. Hydrothermal eruptions may be triggered by the pressure drop associated with fault rupture. (c). Transitory condition in which a high-flux open conduit is generated above the level of dike intrusion. Hydrothermal and hydromagmatic eruptions may be triggered by the dike intrusion. The distribution of minerals that results from boiling is shown on the right margin of diagrams (b) and (c). (Simmons and Browne, 2000). BPD = boiling point for depth temperature. For both (b) and (c), the high-flux conduits conducive to boiling can be located anywhere within the alteration halo.

ore genesis. At Broadlands-Ohaaki, NE-SW–striking structurally controlled quartz and adularia alteration and vein mineralization are forming at <1-km depth in a boiling upflow zone in the northwest part of the system; however, the along strike extent is <1 km as controlled by the overall geometry of the plume structure (Fig. 3), and no significant subsurface precious metal mineralization has been found yet. At Waiotapu, the Champagne Pool lies within a cluster of hydrothermal eruption vents lying just outside the perimeter of the Reporoa caldera. While the current discharge of hot water is modest (~10 kg/s), it contains the highest chloride concentration indicating development of a vertical flow path with high permeability, which taps the deepest known water in the system (Hedenquist, 1991). Moreover, as discussed by Hedenquist and Henley (1985), hydrothermal transport and deposition of precious metals associated with boiling conditions suggest that an epithermal environment underlies this part of the geothermal field.

Concluding Statement

The tempo and range of hydrothermal, magmatic, and tectonic processes in the central Taupo Volcanic Zone are exceptional (Bibby et al., 1995; Hochstein, 1995; Rowland et al., 2010; Wilson et al., 2010b). Interactions between these processes produce inherent variability in the nature and evolution of hydrothermal flow paths, hydrothermal alteration, and the potential sites of epithermal mineralization. Thus, each geothermal system is unique. Fluid-flow paths are complex and difficult to predict, but they are also self-regulating in so far as upflow in the geothermal system is seemingly sustained for long periods of time, because over the long term (>10,000 years), hydrothermal convection is the most efficient means of dissipating the magmatic thermal energy from midcrustal levels. However, the thermal budget is occasionally overwhelmed through rapid accumulation of melt and the result is a volcanic eruption. In the continuum of heat and mass transfer processes, volcanism and steady-state hydrothermal convection are end members. The hydrothermal flow conditions conducive to epithermal mineralization lie in between these end members, because focused fluid discharge is more efficient as a heat transfer mechanism than the distributed hydrothermal flow of the steady state. Using a production well as an analogy, such high-flux conduits provide an efficient means of transferring a large amount of thermal energy per unit time. Mineral deposition limits high flow periods to short time intervals. Spasmodic cycles of vein opening via tectonism, dike intrusion, and/or volcanic eruption, followed by mineral sealing is a key attribute of epithermal ore formation. Another key factor is the availability of precious metals and metal-transporting ligands, which is strongly dependent on magmatic processes and possibly variable over the life time of the system. The complexity of these ore-forming controls supports the notion that epithermal deposits are self-organized phenomena whose formation is a consequence of structurally localized perturbations within crustal-scale geothermal systems that induce rapid mineral deposition in high-permeability fluid-flow regimes (Henley and Berger, 2000). It is not surprising that epithermal orebody geometries are diverse and unpredictable in their occurrence. But they are not freaks of nature, rather they are simply products of highly efficient periods of hydrothermal heat and mass transfer that utilize whatever permeability structure avails the flow of heat to the surface. The capability for high fluid-flow conditions to develop is a feature of all high-temperature geothermal systems, and thus all systems are potential sites of epithermal ore formation.

Acknowledgments

This work was funded by the New Zealand Foundation of Research, Science and Technology, Minerals and Geothermal Programs. Thanks to Patrick Browne for comments in the completion of this manuscript. JR particularly thanks Rick Sibson, whose guidance during her doctoral studies helped in the development of some of the ideas presented here. This manuscript benefited from useful reviews by Steven Micklethwaite, Eric Nelson, Jonathan Caine, and David John.

REFERENCES

Acocella, V., Spinks, K., Cole, J., and Nicol, A., 2003, Oblique back arc rifting of Taupo Volcanic Zone, New Zealand: Tectonics, v. 22, doi: 10.1029 / 2002TC001447.

Anderson, H., Smith, E., and Robinson, R., 1990, Normal faulting in a back arc basin: Seismological characteristics of the March 2, 1987, Edgecumbe, New Zealand, earthquake: Journal of Geophysical Research, v. 95, p. 4709–4723.

Annen, C., Blundy, J.D., and Sparks, R.S.J., 2006. The genesis of intermediate and silicic magmas in deep crustal hot zones: Journal of Petrology, v. 47, p. 505–539.

Berger, B.R., Tingley, J.V., and Drew, L.J., 2003, Structural localization and origin of compartmentalized fluid flow, Comstock Lode, Virginia City, Nevada: Economic Geology, v. 98, p. 387–408.

Berkowitz, B., 2002, Characterizing flow and transport in fractured geological media: A review: Advances in Water Resources, v. 25, p. 861–884.

Berryman, K.R., Villamor, P., Nairn, I.A., Van Dissen, R.J., Begg, J.G., and Lee, J., 2008, Late Pleistocene surface rupture history of the Paeroa Fault, Taupo Rift, New Zealand: New Zealand Journal of Geology and Geophysics, v. 51, p. 135–158.

Bibby, H.M., Caldwell, T.G., Davey, F.J., and Webb, T.H., 1995, Geophysical evidence on the structure of the Taupo Volcanic Zone and its hydrothermal circulation: Journal of Volcanology and Geothermal Research, v. 68, p. 29–58.

Bibby, H.M., Caldwell, T.G., and Risk, G.F., 1998, Electrical resistivity image of the upper crust within the Taupo Volcanic Zone, New Zealand: Journal of Geophysical Research, v. 103, p. 9665–9680.

Bignall, G., 1991, Subsurface stratigraphy and structure of the Orakeikorako and Te Kopia geothermal systems: University of Auckland, New Zealand Geothermal Workshop, 13th, November 1991, Proceedings, p. 199–206.

Bignall, G., and Browne, P.R.L., 1994, Surface hydrothermal alteration and evolution of the Te Kopia geothermal field, New Zealand: Geothermics, v. 23, p. 645–658.

Bignall, G., Sekine, K. And Tsuchiya, N., 2004, Fluid-rock interaction processes in the Te Kopia geothermal field (New Zealand) revealed by SEM-Cl imaging: Geothermics, v. 33, p. 615–635.

Bixley, P.F., Clotworthy, A.W., and Mannington, W.I., 2009, Evolution of the Wairakei geothermal reservoir during 50 years of production: Geothermics, v. 38, p. 145–154.

Björlykke, K., 1997, Lithological control on fluid flow in sedimentary basins, inJamtveit, B., and Yardley, B.W.D., eds., Fluid flow and transport in rocks: Mechanisms and effects: London, Chapman and Hall, p. 15–137.

Brace, W.F., 1980, Permeability of crystalline and argillaceous rocks: International Journal of Rock Mechanics and Mineralogical Science, v. 17, p. 241–251.

Brathwaite, R.L., Wood, C.P., Rosenberg, M.D., and Faure, K., 2002, Porosity and permeability in the basement rocks at the Kawerau and Ohaaki geothermal fields, New Zealand: University of Auckland, New Zealand Geothermal Workshop, 24th, Auckland, November, 2002, Proceedings, p. 49–54.

Brown, K.L., 1986, Gold deposition from geothermal discharges in New Zealand: Economic Geology, v. 81, p. 979–983.

Browne, P.R.L., 1969, Sulfide mineralization in a Broadlands geothermal drill hole, Taupo Volcanic Zone, New Zealand: Economic Geology, v. 64, p.156–159.
——1970, Hydrothermal alteration as an aid to investigating geothermal fields: Geothermics, v. 2, pt. 1, p. 564–570.
——1971, Petrological logs of Broadlands drillholes BR1 to BR25: New Zealand Geological Survey Report 52, 86 p.
——1978, Hydrothermal alteration in active geothermal fields: Annual Review of Earth and Planetary Sciences, v. 6, p. 229–250.
——1979, Minimum age of the Kawerau geothermal field, North Island, New Zealand: Journal of Volcanology and Geothermal Research, v. 6, p. 213–215.
——1989, Investigations of the Rotokawa geothermal field, Taupo Volcanic Zone, New Zealand: Journal of Geothermal Research Society of Japan, v. 11, p. 87–96.
Browne, P.R.L., and Ellis, A.J., 1970, The Ohaaki-Broadlands geothermal area, New Zealand: Mineralogy and related geochemistry: American Journal of Science, v. 269, p. 97–131.
Browne, P.R.L., Graham, I.J., Parker, R.J., and Wood, C.P., 1992, Subsurface andesitic lavas and plutonic rocks in the Rotokawa and Ngatamariki geothermal systems, Taupo Volcanic Zone, New Zealand: Journal of Volcanology and Geothermal Research, v. 51, p. 199–215.
Browne, P.R.L., and Lawless, J.V., 2001, Characteristics of hydrothermal eruptions, with examples from New Zealand and elsewhere: Earth-Science Reviews, v. 52, p. 299–331.
Bryan, C.J., Sherburn, S., Bibby, H.M., Bannister, S.C., and Hurst, A.W., 1999, Shallow seismicity of the central Taupo Volcanic Zone, New Zealand: Its distribution and nature: New Zealand Journal of Geology and Geophysics, v. 42, p. 533–542.
Byerlee, J., 1993, Model for episodic flow of high-pressure water in fault zones before earthquakes: Geology, v. 21, p. 303–306.
Caine, J.S., Evans, J.P., and Forster, C.B., 1996, Fault zone architecture and permeability structure: Geology, v. 24, p. 1025–1028.
Cathles, L.M., Erendi, A.H.J., and Barrie, T., 1997, How long can a hydrothermal system be sustained by a single intrusive event?: Economic Geology, v. 92, p. 766–771.
Charlier, B.L.A., Wilson, C.J.N., Lowenstern, J.B., Blake, S., van Calsteren, P.W., and Davidson, J.P., 2005. Magma generation at a large, hyperactive silicic volcano (Taupo, New Zealand) revealed by U-Th and U-Pb systematics in zircons: Journal of Petrology, v. 46, p. 3–32.
Christenson, B.W., Mroczek, E.K., Kennedy, B.M., van Soest, M.C., Stewart, M.K., and Lyon, G., 2002, Ohaaki reservoir chemistry: Characteristics of an arc-type hydrothermal system in the Taupo Volcanic Zone, New Zealand: Journal of Volcanology and Geothermal Research, v. 115, p. 53–82.
Clark, J.P., and Browne, P.R.L., 1998, Surface alteration between Orakeikorako and Te Kopia thermal area: University of Auckland, New Zealand Geothermal Workshop, 20th, November 1998, Proceedings, p. 271–276.
Clarke, D., Townend, J., Savage, M.K., and Bannister, S., 2009, Seismicity in the Rotorua and Kawerau geothermal systems, Taupo Volcanic Zone, New Zealand, based on improved velocity models and cross-correlation measurements: Journal of Volcanology and Geothermal Research, v. 180, p. 50–66.
Cochrane, G.R., and Wan, T., 1983: Interpretation of structural characteristics of the Taupo Volcanic Zone, New Zealand, from Landsat imagery: International Journal of Remote Sensing, v. 4, p. 111–128.
Collar, R.J., 1985, Hydrothermal eruptions in the Rotokawa geothermal system, Taupo Volcanic Zone, New Zealand: Geothermal Institute, Auckland, New Zealand, University of Auckland, Unpublished report, 96 p.
Collar, R.J., and Browne, P.R.L., 1985, Hydrothermal eruptions at the Rotokawa geothermal field, Taupo Volcanic Zone, New Zealand: University of Auckland, New Zealand Geothermal Workshop, 7th, November 1985, Proceedings, p. 171–175.
Cosgrove, J.W., 1995, The expression of hydraulic fracturing in rocks and sediments: Geological Society Special Publication 92, p. 187–196.
Cox, S.F., 2005, Coupling between deformation, fluid pressures and fluid flow in ore-producing hydrothermal environments: Economic Geology 100th Anniversary Volume, p. 39–75.
——2010, The application of failure mode diagrams for exploring the roles of fluid pressure and stress states in controlling styles of fracture-controlled permeability enhancement in faults and shear zones: Geofluids, v. 10, p. 217–233.
Cox, S.F., Knackstedt, M.A., and Braun, J., 2001, Principles of structural control on permeability and fluid flow in hydrothermal systems: Reviews in Economic Geology, v. 14, p. 1–24.
Crider, J.G., and Pollard, D.D., 1998, Fault linkage: Three-dimensional interaction between echelon normal faults: Journal of Geophysical Research, v. 103, p. 24373–24391.
Curewitz, D., and Karson, J.A., 1997, Structural settings of hydrothermal outflow: Fracture permeability maintained by fault propagation and interaction: Journal of Volcanology and Geothermal Research, v. 79, p. 149–168.
Darby, D.J., and Meertens, C.M., 1995, Terrestrial and GPS measurements of deformation across the Taupo back-arc and Hikurangi forearc regions in New Zealand: Journal of Geophysical Research, v. 100, p. 8221–8232.
Donaldson, I.G., and Grant, M.A., 1981, Heat extraction from geothermal reservoirs, *in* L. Rybach, L., and Muffler, L.J.P., eds., Geothermal systems: Principles and case histories: Chichester, John Wiley and Sons, 371 p.
Dunbar, N.W., Hervig, R.L., and Kyle, P.R., 1989, Determination of pre-eruptive H_2O, F and Cl contents of silicic magmas using melt inclusions: Examples from Taupo volcanic centre, New Zealand: Bulletin of Volcanology, v. 51, p. 177–184.
Ebinger, C.J., and Casey, M., 2001, Continental break-up in magmatic provinces: Aan Ethiopian example: Geology, v. 29, p. 527–530.
Ebinger, C.J., Jackson, J.A., Foster, A.N., and Hayward, N.J., 1999, Extensional basin geometry and the elastic lithosphere: London, Philosophical Transactions of the Royal Society, A, v. 357, p. 741–765.
Elder, J.W., 1981, Geothermal systems: London, Academic Press, 508 p.
Ellis, S.M., Wilson, C.J.N., Bannister, S., Biby, H.M., Heise, W., Wallace, L., and Patterson, N., 2007, A future magma inflation event under the rhyolitic Taupo volcano, New Zealand: Numerical models based on constraints from geochemical, geological, and geophysical data: Journal of Volcanology and Geothermal Research, v. 168, p. 1–27.
Ferrill, D.A., and Morris, A.P., 2001, Displacement gradient and deformation in normal fault systems: Journal of Structural Geology, v. 23, p. 619–638.
Gibbs, A.D., 1984, Structural evolution of extensional basin margins: Journal of the Geological Society, London, v. 141, p. 609–620.
Giggenbach, W.F., 1995, Variations in chemical and isotopic composition of fluids discharged from the Taupo Volcanic Zone, New Zealand: Journal of Volcanology and Geothermal Research, v. 68, p. 89–116.
Giggenbach, W.F., and Glover, R.B., 1992, Tectonic regime and major processes governing the chemistry of water and gas discharges from the Rotorua geothermal field, New Zealand: Geothermics, v. 21, p. 121–140.
Giggenbach, W.F., Sheppard, D.S., Robinson, B.W., Stewart, M.K., and Lyon, G.L., 1994, Geochemical structure and position of the Waiotapu geothermal field, New Zealand: Geothermics, v. 23, p. 599–644.
Grange, L.I., 1937, The geology of the Rotorua-Taupo subdivision: Bulletin of the New Zealand Geological Survey (n.s), v. 37, 138 p.
Grant, M.A., and Bixley, P.F., 2011, Geothermal reservoir engineering: Burlington, Academic Press, 2nd ed., 359 p.
Grant, M.A., Donaldson, I.G., and Bixley, P.F., 1982, Geothermal reservoir engineering: New York, Academic Press, 369 p.
Grant-Taylor, T.L., and Rafter, T.A., 1971, New Zealand radiocarbon age measurement – 6: New Zealand Journal of Geology and Geophysics, v. 14, p. 364.
Gravley, D.M., Wilson, C.J.N., Leonard, G.S., and Cole, J.W., 2007, Double trouble: Paired ignimbrite eruptions and collateral subsidence in the Taupo Volcanic Zone, New Zealand: Geological Society of America Bulletin, v. 119, p. 18–30.
Grieve, P.L., Corbett, G.J., and Leach, T.M., 2006, Exploration at Ohakuri North epithermal Au-Ag prospect, Taupo Volcanic Zone: Australian Institute of Mining and Metallurgy Monograph 25, p. 197–202.
Grimes, S., Rickard, D., Hawkesworth, C., van Calsteren, P., and Browne, P., 1998, A U-Th calcite isochron age from an active geothermal field in New Zealand: Journal of Volcanology and Geothermal Research, v. 81, p. 327–333.
Grindley, G.W., and Browne, P.R.L., 1968, Subsurface geology of the Broadlands geothermal field: New Zealand Geological Survey Report, 34 p.
—1976, Structural and hydrological factors controlling the permeabilities of some hot-water geothermal fields: U.N. Symposium on Development and Use of Geothermal Resources, 2nd, San Francisco, 1975, Proceedings, p. 377–386.
Grindley, G.W., Mumme, T.C., and Kohn, B.P., 1994, Stratigraphy, paleomagnetism, geochronology and structure of silicic volcanic rocks, Waiotapu/Paeroa Range area, New Zealand: Geothermics, v. 23, p. 473–499.
Hanano, M., 2004, Contribution of fractures to formation and production of geothermal resources: Renewable and Sustainable Energy Reviews, v. 8, p. 223–236.

Harrison, A.J., and White, R.S., 2004, Crustal structure of the Taupo Volcanic Zone, New Zealand: Stretching and igneous intrusion: Geophysical Research Letters, v. 31, L13615, doi:10.1029/2004GL019885.

——2006, Lithospheric structure of an active backarc basin: the Taupo Volcanic Zone, New Zealand: Geophysical Journal International, v. 167, p. 968–990.

Hedenquist, J.W., 1990, The thermal and geochemical structure of the Broadlands-Ohaaki geothermal System, New Zealand: Geothermics, v. 19, p. 151–185.

——1991, Boiling and dilution in the shallow portion of the Waiotapu geothermal system, New Zealand: Geochimica et Cosmochimica Acta, v. 55, p. 2753–2765.

Hedenquist, J.W., and Browne, P.R.L., 1989, The evolution of the Waiotapu geothermal system, New Zealand, based on the chemical and isotopic composition of its fluids, minerals and rocks: Geochimica et Cosmochimica Acta, v. 53, p. 2235–2257.

Hedenquist, J.W., and Henley, R.W., 1985, Hydrothermal eruptions in the Waiotapu geothermal system, New Zealand: Their origin, associated breccias, and relation to precious metal mineralization: Economic Geology, v. 80, p. 1640–1668.

Heise, W., Bibby, H.M., Caldwell, T.G., Bannister, S.C., Ogawa, Y., Takakura, S., and Uchida, T., 2007, Melt distribution beneath a young continental rift: the Taupo Volcanic Zone, New Zealand: Geophysical Research Letters, v. 34, L14313, doi:10.1029/2007GL029629.

Heise, W., Caldwell, T.G., Bibby, H.M., and Bannister, S.D., 2008, Three-dimensional modeling of magnetotelluric data from the Rotokawa geothermal field, Taupo Volcanic Zone, New Zealand: Geophysical Journal International, v. 173, p. 740–750.

Henley, R.W., 1985, The geothermal framework for epithermal deposits: Reviews in Economic Geology, v. 2, p. 1–24.

Henley, R.W., and Adams, D.P.M., 1992, Strike-slip-fault reactivation as a control on epithermal vein style gold mineralization: Geology, v. 20, p. 443–446.

Henley, R.W., and Berger, B.R., 2000, Self-ordering and complexity in epizonal mineral deposits: Annual Review of Earth and Planetary Sciences, v. 28, p. 669–719.

Henley, R.W., and Ellis, A.J., 1983, Geothermal systems ancient and modern: A geochemical review: Earth-Science Reviews, v. 19, p. 1–50.

Henneberger, R.C., and Browne, P.R.L., 1988, Hydrothermal alteration and evolution of the Ohakuri hydrothermal system, Taupo Volcanic Zone, New Zealand: Journal of Volcanology and Geothermal Research, v. 34, p. 211–231.

Henrys, S.A., and Hochstein, M.P., 1990, Geophysical structure of the Broadlands-Ohaaki geothermal field (New Zealand): Geothermics, v. 19, p. 129–150.

Hildreth, W., 1981, Gradients in silicic magma chambers: Implications for lithospheric magmatism: Journal of Geophysical Research, v. 86, p. 10153–10192.

Hildreth, W., and Moorbath, S., 1988, Crustal contributions to arc magmatism in the Andes of central Chile: Contributions to Mineralogy and Petrology, v. 98, p. 455–489.

Hochstein, M.P., 1995, Crustal heat transfer in the Taupo Volcanic Zone (New Zealand): Comparison with other volcanic arcs and explanatory heat source models: Journal of Volcanology and Geothermal Research, v. 68, p. 117–151.

Houghton, B.F., Wilson, C.J.N., McWilliams, M.O., Lanphere, M.A., Weaver, S.D., Briggs, R.M., and Pringle, M.S., 1995, Chronology and dynamics of a large silicic magmatic system: central Taupo Volcanic Zone, New Zealand: Geology, v. 23, p. 13–16.

Hurst, A.W., Bibby, H.M., and Robinson, R.R., 2002, Earthquake focal mechanisms in the central Taupo Volcanic Zone and their relation to faulting and deformation: New Zealand Journal of Geology and Geophysics, v. 45, p. 527–536.

Keam, R.F., 1981, Frying Pan Lake provisional bathymetry, 1:500: New Zealand Oceanographic Institute, Department of Scientific and Industrial Research Miscellaneous Series 53.

Knott, S.D., 1993, Fault seal analysis in the North Sea: American Association of Petroleum Geologists Bulletin, v. 77, p. 778–792.

Knott, S.D., Beach, A., Brockbank, P.J., Lawson Brown, J., McCallum, J.E., and Welbon, A.I., 1996 Spatial and mechanical controls on normal fault populations: Journal of Structural Geology, v. 18, p. 359–372.

Koerner, A., Kissling, E., and Miller, S.A., 2004, A model of deep crustal fluid flow following the Mw = 8.0 Antofagasta, Chile, earthquake: Journal of Geophysical Research, v. 109, doi: 10.1029/2003JB002816. B06307.

Krupp, R.E., and Seward, T.M., 1987, The Rotokawa geothermal system, New Zealand—an active epithermal gold-depositing environment: Economic Geology, v. 82, p. 1109–1129.

Lamarche, G., Barnes, P.M., and Bull, J.M., 2006, Faulting and extension rate over the last 20,000 years in the offshore Whakatane graben, New Zealand continental shelf: Tectonics, v. 25, doi: 10.1029/2005TC001886.

Le Turdu, C., Richert, J.P., Xavier, J.-P., Renaut, R.W., Tiercelin, J.-J., Rolet, J., Lezzar, K.E., and Coussement, C., 1999, Influence of preexisting oblique discontinuities on the geometry and evolution of extensional fault patterns: Evidence from the Kenya rift using SPOT imagery: American Association of Petroleum Geologists Studies in Geology, v. 44, p. 173–191.

Lister, C.R.B., 1974, On the penetration of water into hot rock: Geophysical Journal of the Royal Astronomical Society, v. 39, p. 465–509.

Liu, Y., Anderson, A.T., Wilson, C.J.N., Davis, A.M., and Steele, I.M., 2006, Mixing and differentiation in the Oruanui rhyolitic magma, Taupo, New Zealand: Evidence from volatiles and trace elements in melt inclusions: Contributions to Mineralogy and Petrology, v. 151, p. 71–87.

Lloyd, E.F., 1959, The hot springs and hydrothermal eruptions of Waiotapu: New Zealand Journal of Geology and Geophysics, v. 2, p. 141–176.

——1972, Geology and hotsprings of Orakeikorako: New Zealand Geological Survey Bulletin, v. 85, 183 p.

McNabb, A., 1975, Geothermal physics: Wellington, New Zealand, Department of Scientific and Industrial Research, Applied Mathematics Division, Technical Report 32, 37 p.

Manning, C.E., and Ingebritsen, S.E., 1999, Permeability of the continental crust: Implications of geothermal data and metamorphic systems: Reviews of Geophysics, v. 37, p. 127–150.

Mannington, W., O'Sullivan, M., and Bullivant, D., 2004, Computer modelling of the Wairakei-Tauhara geothermal system, New Zealand: Geothermics, v. 33, p. 401–419.

Martin, R., Mildenhall, D.C., Browne, P.R.L., and Rodgers, K.A., 2000, The age and significance of in situ sinter at the Te Kopia thermal area, Taupo Volcanic Zone, New Zealand: Geothermics, v. 29, p. 367–375.

Micklethwaite, S., 2009, Mechanisms of faulting and permeability enhancement during epithermal mineralization: Cracow goldfield, Australia: Journal of Structural Geology, v. 31, p. 288–300.

Micklethwaite, S., Sheldon, H.A., and Baker, T., 2010, Active fault and shear processes and their implications for mineral deposit formation and discovery: Journal of Structural Geology, v. 32, p. 151–165.

Miller, S.A., Colletini, C., Chiaraluce, L., Cocco, M., Barchi, M., and Kaus, B.J.P., 2004, Aftershocks driven by a high-pressure CO_2 source at depth: Nature, v. 427, p. 724–727.

Ministry of Works and Development, 1977, Broadlands geothermal field investigation report: Wellington, New Zealand, Unpublished internal report, 236 p.

Morley, C.K., 1999, Influence of preexisting fabrics on rift structure: American Association of Petroleum Geologists Studies in Geology, v. 44, p. 151–160.

Morley, C.K., Nelson, R.A., Patton, T.L., and Munn, S.G., 1990, Transfer zones in the East African rift system and their relevance to hydrocarbon exploration in rifts: American Association of Petroleum Geologists Bulletin, v. 74, p. 1234–1253.

Nairn, I.A., and Cole, J.W., 1981, Basalt dikes in the 1886 Tarawera rift: New Zealand Journal of Geology and Geophysics, v. 24, p. 585–592.

Nairn, I.A., Wood, C.P., and Bailey, R.A., 1994, The Reporoa caldera, Taupo Volcanic Zone: Source of the Kaingaroa ignimbrites: Bulletin of Volcanology, v. 56, p. 529–637.

Nairn, I.A., Shane, P.R., Cole, J.W., Leonard, G.J., Self, S., and Pearson, N., 2004, Rhyolite magma processes of the ~AD 1315 Kaharoa eruption episode, Tarawera volcano, New Zealand: Journal of Volcanology and Geothermal Research, v. 131, p. 265–294.

Nairn, I.A., Hedenquist, J.W., Villamor, P., Berryman, K.R., and Shane, P.A., 2005, The ~AD1315 Tarawera and Waiotapu eruptions, New Zealand: Contemporaneous rhyolite and hydrothermal eruptions driven by an arrested basalt dike system?: Bulletin of Volcanology, v. 67, p. 186–193.

Neuzil, C.E., 1995, Abnormal pressures as hydrodynamic phenomena: American Journal of Science, v. 295, p. 742–786.

Nortje, G.S., Rowland, J.V., Sporli, K.B., Blenkinsop, T.G., and Rabone, S.D.C., 2006, Vein deflections and thickness variations of epithermal quartz veins as indicators of fracture coalescence: Journal of Structural Geology, v. 28, p. 1396–1405.

Omori, F., 1894, On the aftershocks of earthquakes: Imperial University of Tokyo, Journal of the College of Science, v. 7, p. 111–200.

Pollard, D.D., Delaney, P.T., Duffield, W.A., Endo. E.T., and Okamura, A.T., 1983, Surface deformation in volcanic rift zones: Tectonophysics, v. 94, p. 541–584.

Pope, J.G., Brown, K.L., and McConchie, D.M., 2005, Gold concentrations in springs at Waiotapu, New Zealand: Implications for precious metal deposition in geothermal systems: Economic Geology, v. 100, p. 677–687.

Renders, P.J., and Seward, T.M., 1989, The adsorption of thio gold (I) complexes by amorphous As_2S_3 and Sb_2S_3 at 25 and 90°C: Geochimica et Cosmochimica Acta, v. 40, p.379–399.

Reyes, A.G., Trompetter, W.J., Britten, K., and Searle, J., 2003, Mineral deposits in the Rotokawa geothermal pipelines, New Zealand: Journal of Volcanology and Geothermal Research, v. 119, p. 215–239.

Ring, U., 1994, The influence of preexisting structure on the evolution of the Cenozoic Malawi rift (East African rift system): Tectonics, v. 13, p. 313–326.

Rosendahl, B.R., Reynolds, D.J., Lorber, P.M., Burgess, C.F., McGill, J., Scott, D., Lambiase, J.J., and Derksen, S.J., 1986, Structural expressions of rifting: Lessons from Lake Tanganyika, Africa: Geological Society Special Publication 25, p. 29–43.

Rowland, J.V., and Sibson, R.H., 2001, Extensional fault kinematics within the Taupo Volcanic Zone, New Zealand: Soft-linked segmentation of a continental rift system: New Zealand Journal of Geology and Geophysics, v. 44, p. 271–284.

——2004, Structural controls on hydrothermal flow in a segmented rift system, Taupo Volcanic Zone, New Zealand: Geofluids, v. 4, p. 259–283.

Rowland, J.V., Baker, E., Ebinger, C.J., Keir, D., Kidane, T., Biggs, J., Hayward, N., and Wright, T.J., 2007, Fault growth at a nascent slow-spreading ridge: 2005 Dabbahu rifting episode, Afar: Geophysical Journal International, v. 171, p. 1226–1246.

Rowland, J.V., Wilson, C.J.N., and Gravley, D.M., 2010, Spatial and temporal variations in magma-assisted rifting, Taupo Volcanic Zone, New Zealand: Journal of Volcanology and Geothermal Research, v. 190, p. 89–108.

Sanematsu, K., Watanabe, K., Duncan, R. A., and Izawa, E., 2006, The history of vein formation determined by $^{40}Ar/^{39}Ar$ dating of adularia in the Hosen-1 vein at the Hishikari epithermal deposit, Japan: Economic Geology, v. 101, p. 685–698

Shane, P., Martin, S.B., Smith, V.C., Beggs, K.F., Darragh, M.B., Cole, J.W., and Nairn, I.A., 2007, Multiple rhyolite magmas and basalt injection in the 17.7 ka Rerewhakaaitu eruption episode from Tarawera volcanic complex, New Zealand: Journal of Volcanology and Geothermal Research, v. 164, p. 1–26.

Shane, P., Nairn, I.A., Smith, V.C., Darragh, M., Beggs, K., and Cole, J.W., 2008, Silicic recharge of multiple rhyolite magmas by basaltic intrusion during the 22.6 ka Okareka eruption episode, New Zealand: Lithos, v. 103, p. 527–549.

Sheppard, D.S., and Lyon, G.L., 1984, Geothermal fluid chemistry of the Orakeikorako field, New Zealand: Journal of Volcanology and Geothermal Research, v. 22, p. 329–349.

Sherburn, S., 1992, Characteristics of earthquake sequences in the central volcanic region: New Zealand Journal of Geology and Geophysics, v. 35, p. 57–68.

Sherburn, S., Bannister, S., and Bibby, H., 2003, Seismic velocity structure of the central Taupo Volcanic Zone, New Zealand, from local earthquake tomography: Journal of Volcanology and Geothermal Research, v. 122, p. 69–88.

Sibson, R.H., 1985, A note on fault reactivation: Journal of Structural Geology, v. 7, p. 751–754.

——1992, Implications of fault-valve behavior for rupture nucleation and recurrence: Tectonophysics, v. 211, p. 283–293.

——1998, Brittle failure mode plots for compressional and extensional tectonic regimes: Journal of Structural Geology, v. 20, p. 655–660.

——2000, Fluid involvement in normal faulting: Journal of Geodynamics, v. 29, p. 469–499.

——2001, Seismogenic framework for hydrothermal transport and ore deposition: Reviews in Economic Geology, v. 14, p. 25–50.

Sibson, R.H., and Rowland, J.V., 2003, Stress, fluid pressure and structural permeability in seismogenic crust, North Island, New Zealand: Geophysical Journal International, v. 154, p. 584–594.

Sillitoe, R.H., 1993, Epithermal models: Genetic types, geometrical controls and shallow features: Geological Association of Canada Special Paper 40, p. 403–417.

Simmons, S.F., and Browne, P.R.L., 2000, Hydrothermal minerals and precious metals in the Broadlands-Ohaaki geothermal system: Implications for understanding low-sulfidation epithermal environments: Economic Geology, v. 95, p. 971–999.

Simmons, S.F., and Brown, K.L., 2007, The flux of gold and related metals through a volcanic arc, Taupo Volcanic Zone, New Zealand: Geology, v. 35, p. 1099–1102.

Simmons, S.F. and Christenson, B.W., 1994, Origins of calcite in a boiling geothermal system: American Journal of Science, v. 294, p. 361–400.

Simmons, S.F., Keywood, M., Scott, B.J., and Keam, R.F. 1993, Irreversible change of the Rotomahana-Waimangu hydrothermal system (New Zealand) as a consequence of a volcanic eruption: Geology, v. 21, p. 643–646.

Simmons, S.F., Stewart, M.K., Robinson, B.W., and Glover, R.B., 1994, The chemical and isotopic compositions of thermal waters at Waimangu, New Zealand: Geothermics, v. 23, p. 539–553.

Simmons, S.F., White, N.C., and John, D., 2005, Geological characteristics of epithermal precious and base metal deposits: Economic Geology 100th Anniversary Volume, p. 485–522.

Simmons, S.F., Simpson, M.P., and Reynolds, T.J., 2007, The significance of clathrates in fluid inclusions and the evidence for overpressuring in the Broadlands-Ohaaki geothermal system, New Zealand: Economic Geology, v. 102, p. 127–135.

Simpson, M.P., and Mauk, J.L., 2007, The Favona epithermal gold-silver deposit, Waihi, New Zealand: Economic Geology, v. 102, p. 817–839.

Smith, E.G.C., and Oppenheimer, C.M.M., 1989, The Edgecumbe earthquake sequence: 1987 February 21 to March 18: New Zealand Journal of Geology and Geophysics, v. 32, p. 31–42.

Smith, E.G.C., Williams, T.D., and Darby, D.J., 2007, Principal component analysis and modeling of the subsidence of the shoreline of Lake Taupo, New Zealand, 1983–1999: Evidence for dewatering of a magmatic intrusion?: Journal of Geophysical Research, v. 112, doi: 10.1029/2006BJ004652.

Smith, V.C., Shane, P., and Nairn, I.A., 2004, Reactivation of a rhyolitic magma body by new rhyolitic intrusion before the 15.8 ka Rotorua episode: Implications for magma storage in the Okataina Volcanic Centre, New Zealand: Journal of the Geological Society, London, v. 161, p. 757–772.

——2005, Trends in rhyolite geochemistry, mineralogy, and magma storage during the last 50ky at Okataina and Taupo Volcanic Centres, Taupo Volcanic Zone, New Zealand: Journal of Volcanology and Geothermal Research, v. 148, p. 372–406.

Stagpoole, V.M., and Bibby, H.M., 1998, Electrical resistivity map of the Taupo Volcanic Zone, New Zealand, nominal array spacing 500 m, 1:250,000, version 1.0: Lower Hutt, New Zealand, Institute of Geological and Nuclear Sciences Ltd. Geophysical Map 11.

Stern, T.A., 1986, Geophysical studies of the upper crust within the Central Volcanic region, New Zealand: Royal Society of New Zealand Bulletin, v. 23, p. 92–111.

Stimac, J., Powell, T.S., and Golla, G.U., 2004, Porosity and permeability of the Tiwi geothermal field, Philippines, based on continuous and spot core measurements: Geothermics, v. 33, p. 87–107.

Stimac, J., Nordquist, G, Suminar, A., and Sirad-Azwar, L., 2008, An overview of the Awibengkok geothermal system, Indonesia: Geothermics, v. 37, p. 300–331.

Stratford, W.R., and Stern, T.A., 2004, Strong seismic reflections and melts in the mantle of a continental back-arc basin: Geophysical Research Letters, v. 31, L06622, doi:10.1029/2003GL019232.

——2006, Crust and upper mantle structure of a continental backarc, Central North Island, New Zealand: Geophysical Journal International, v. 166, p. 469–484.

Sutton, F.M., and McNabb, A., 1977, Boiling curves at Broadlands geothermal field, New Zealand: New Zealand Journal of Science, v. 20, p. 333–337.

Talwani, P., and Acree, S., 1984, Pore pressure diffusion and the mechanism of reservoir-induced seismicity: Pure and Applied Geophysics, v. 122, p. 947–965.

Thompson, G.E.K., 1963, Some physical measurements in the Waiotapu area: New Zealand Department of Scientific and Industrial Research Bulletin: v. 155, p. 59–74.

Townend, J., and Zoback, M.D., 2000, How faulting keeps the crust strong: Geology, v. 28, p. 399–402.

Villamor, P., and Berryman, K., 2006, Evolution of the southern termination of the Taupo rift: New Zealand Journal of Geology and Geophysics, v. 49, p. 23–37.

Wallace, L.M., Beavan, J., McCaffrey, R., and Darby, D.J., 2004, Subduction zone coupling and tectonic block rotations in the North Island, New Zealand: Journal of Geophysical Research, v. 109, B12406, doi:10.1029/2004JB003241.

Wan, T., and Hedenquist, J.W., 1981, A reassessment of the structural control of the Broadlands geothermal field, New Zealand: University of Auckland, New Zealand Geothermal Workshop, 3rd, November 1981, Proceedings, p. 195–202.

Weissberg, B.G., 1969, Gold-silver ore-grade precipitates from New Zealand thermal waters: Economic Geology, v. 64, p. 95–108.

White, S.P., and Mroczec, E.K., 1998, Permeability changes during the evolution of a geothermal field due to the dissolution and precipitation of quartz: Transport in Porous Media, v. 33, p. 81–101.

Wibberley, C.A.J., and Shimamoto, T., 2003, Internal structure and permeability of major strike-slip fault zones: the Median Tectonic Line in Mie Prefecture, Southwest Japan: Journal of Structural Geology, v. 25, p. 59–78.

Wilson, C.J.N., Houghton, B.F., McWilliams, M.O., Lanphere, M.A., Weaver, S.D., and Briggs, R.M., 1995, Volcanic and structural evolution of Taupo Volcanic Zone, New Zealand: A review: Journal of Volcanology and Geothermal Research, v. 68, p. 1–28.

Wilson, C.J.N., Charlier, B.L.A., Rowland, J.V., and Browne, P.R.L., 2010a, U-Pb dating of zircon in subsurface, hydrothermally altered pyroclastic deposits and implications for subsidence in a magmatically active rift: Taupo Volcanic Zone, New Zealand: Journal of Volcanology and Geothermal Research, v. 191, p. 69–78.

Wilson, C.J.N., Gravley, D.M., Leonard, G.S., and Rowland, J.V., 2010b, Volcanism in the central Taupo Volcanic Zone, New Zealand: Tempo, styles and controls: Geological Society of London Special Publication 2, p. 225–247.

Wood, C.P., 1983, Petrological logs of drillholes BR 26 to BR 40: Broadlands geothermal field: New Zealand, NZGS Report 108, 49 p.

—1994, Aspects of the geology of Waimangu, Waiotapu, Waikite and Reporoa geothermal systems, Taupo Volcanic Zone, New Zealand: Geothermics, v. 23, p. 401–421.

Wood, C.P., Brathwaite, R.L., and Rosenberg, M.D., 2001, Basement structure, lithology and permeability at Kawerau and Ohaaki geothermal fields, New Zealand: Geothermics, v. 30, p. 461–481.